

Possible Involvement of Phosphorylation of Occludin in Tight Junction Formation

Akira Sakakibara,*[‡] Mikio Furuse,* Mitinori Saitou,* Yuhko Ando-Akatsuka,* and Shoichiro Tsukita*

*Department of Cell Biology, Faculty of Medicine, Kyoto University, Sakyo-ku, Kyoto 606, Japan; and [‡]Department of Physiological Sciences, School of Life Science, The Graduate University for Advanced Studies, Myodaiji, Okazaki, Aichi 444, Japan

Abstract. Occludin is an integral membrane protein localizing at tight junctions in epithelial and endothelial cells. Occludin from confluent culture MDCK I cells resolved as several (>10) bands between 62 and 82 kD in SDS-PAGE, of which two or three bands of the lowest M_r were predominant. Among these bands, the lower predominant bands were essentially extracted with 1% NP-40, whereas the other higher M_r bands were selectively recovered in the NP-40-insoluble fraction. Alkaline phosphatase treatment converged these bands of occludin both in NP-40-soluble and -insoluble fractions into the lowest M_r band, and phosphoamino acid analyses identified phosphoserine (and phosphothreonine weakly) in the higher M_r bands of occludin. These findings indicated that phosphorylation causes an upward shift of occludin bands and that highly phosphorylated occludin resists NP-40 extraction. When cells were grown in low Ca medium, almost all occludin was NP-40 soluble. Switching from low to normal Ca medium increased the amount of NP-40-insoluble occludin within

10 min, followed by gradual upward shift of bands. This insolubilization and the band shift correlated temporally with tight junction formation detected by immunofluorescence microscopy. Furthermore, we found that the anti-chicken occludin mAb, Oc-3, did not recognize the predominant lower M_r bands of occludin (non- or less phosphorylated form) but was specific to the higher M_r bands (phosphorylated form) on immunoblotting. Immunofluorescence microscopy revealed that this mAb mainly stained the tight junction proper of intestinal epithelial cells, whereas other anti-occludin mAbs, which can recognize the predominant lower M_r bands, labeled their basolateral membranes (and the cytoplasm) as well as tight junctions. Therefore, we conclude that non- or less phosphorylated occludin is distributed on the basolateral membranes and that highly phosphorylated occludin is selectively concentrated at tight junctions as the NP-40-insoluble form. These findings suggest that the phosphorylation of occludin is a key step in tight junction assembly.

OCCLUDIN is an integral membrane protein localizing at tight junctions in epithelial and endothelial cells. It was first identified in the chicken using monoclonal antibodies (Furuse et al., 1993) and most recently in mammalian species (Ando-Akatsuka et al., 1996; Saitou et al., 1997). Occludin consists of four transmembrane domains, three cytoplasmic domains (long COOH-terminal and short NH₂-terminal domains, and one short intracellular turn), and two extracellular loops. Among these domains, the first extracellular loop is characterized by an unusually high content of tyrosine and glycine residues (~60%). The sequence of the COOH-terminal, ~150 amino acids, is relatively conserved among species, and it is reportedly bound to ZO-1, a 220-kD tight junction-asso-

ciated, lethal(1)discs large-1 (dlg)-like peripheral membrane protein (Stevenson et al., 1986; Anderson et al., 1988; Itoh et al., 1993; Willott et al., 1993; Furuse et al., 1994). Together with other tight junction undercoat-constitutive proteins such as ZO-2 (Gumbiner et al., 1991; Jesaitis and Goodenough, 1994), cingulin (Citi et al., 1988), 7H6 antigen (Zhong et al., 1993), and symplekin (Keon et al., 1996), ZO-1 appears to link occludin to the actin-based cytoskeleton (Madara, 1987; Citi, 1993; Gumbiner, 1993).

Tight junctions play the dual roles of barrier and fence in epithelial and endothelial cells. They create the primary barrier to the diffusion of solutes through the paracellular pathway and maintain cell polarity as a boundary between the apical and basolateral plasma membrane domains (for reviews see Schneeberger and Lynch, 1992; Gumbiner, 1987, 1993). As the morphological counterpart of the barrier function, in thin section electron microscopy, tight junctions appear as a series of discrete sites of apparent fusion, involving the outer leaflet of the plasma membrane of adjacent cells (Farquhar and Palade, 1963). Occludin is

Please address all correspondence to Dr. Shoichiro Tsukita, Department of Cell Biology, Kyoto University, Faculty of Medicine, Konoe-Yoshida, Sakyo-ku, Kyoto 606, Japan. Tel.: (81) 75-753-4372; Fax: (81) 75-753-4660; E-mail: htsukita@mfour.med.kyoto-u.ac.jp

localized at these apparent fusion points (Furuse et al., 1993), and its overexpression results in transepithelial electric resistance (TER)¹ elevation (Balda et al., 1996; McCarthy et al., 1996). Furthermore, most recently a synthetic peptide corresponding to the second extracellular loop of chicken occludin was reported to perturb the tight junction barrier in a very specific manner (Wong and Gumbiner, 1997). In freeze fracture electron microscopy, tight junctions appear as a set of continuous, anastomosing intramembranous particle strands, which are thought to work as a fence in the plasma membranes. Immunoelectron microscopic studies of freeze fracture replicas revealed that occludin is at least one of the major components of the tight junction strand itself (Fujimoto, 1995; Furuse et al., 1996), and a truncated occludin lacking its COOH-terminal cytoplasmic domain works in a dominant-negative manner, resulting in the destruction of a fence between apical and basolateral membrane domains (Balda et al., 1996). These findings indicate that occludin is a key component of tight junctions structurally as well as functionally.

The functions of tight junctions are dynamically regulated, but the molecular mechanism remains elusive. For example, knowledge of how the permeability of endothelial cells is elevated during an inflammatory reaction (Lum and Malik, 1994) and how the permeability of intestinal epithelial cells is controlled during absorption (Madara and Pappenheimer, 1987) is still fragmentary. Occludin is possibly involved in this regulation mechanism of tight junctions at two distinct levels: transcriptional and posttranslational. Indeed, occludin expression appears to be tightly regulated at the transcriptional level. Occludin mRNA is detected in epithelial and endothelial cells by Northern blotting but not in fibroblastic cells (Saitou et al., 1997).

In connection with posttranslational modification, it is noteworthy that chicken, as well as mammalian occludin, resolves on SDS-PAGE as several closely migrating bands, the smallest of which is the most intense (Furuse et al., 1993; Saitou et al., 1997). In this study we show that serine/threonine-phosphorylation shifted the occludin band upward as multiple bands and that highly phosphorylated occludin resists detergent extraction. Calcium switch experiments revealed that tight junction formation is accompanied by the insolubilization and phosphorylation of occludin. Furthermore, we found that one of our mAbs raised against chicken occludin is specific for phosphorylated occludin and that this mAb mainly stained the tight junction proper. These findings suggest that phosphorylation is essential for occludin to form functional tight junctions.

Materials and Methods

Antibodies and Cells

Rat anti-mouse occludin mAb (MOC37) and rabbit anti-mouse occludin pAbs (F4 and F5) were raised against the cytoplasmic domain of mouse occludin produced in *Escherichia coli* (Saitou et al., 1997). Rat anti-chicken occludin mAbs (Oc-1, Oc-2, Oc-3) and a mouse anti-rat ZO-1 mAb (T8-754) were raised and characterized as described (Itoh et al., 1991; Furuse et al., 1993, 1996). Anti-chicken occludin pAb (F44) was

raised in rabbits against the COOH-terminal cytoplasmic domain of chicken occludin that was produced in *E. coli*.

MDCK I cells were grown in minimal essential medium (MEM) supplemented with 5% FCS. Mouse epithelial cells, MTD-1A, were cultured in DMEM containing 10% FCS, and T84 human epithelial cells were grown in a 1:1 mixture of DMEM and Ham's F-12 medium containing 5% FCS.

Immunoprecipitation

MDCK I cells were cultured on two 24-mm filters (Transwell; Corning Costar Corp., Cambridge, MA), washed three times with ice-cold PBS, and then lysed in 500 μ l of ice-cold NP-40-IP buffer (25 mM Hepes/NaOH, pH 7.4, 150 mM NaCl, 4 mM EDTA, 25 mM NaF, 1% NP-40, 1 mM Na₃VO₄, 1 mM APMSF, 10 μ g/ml leupeptin, 10 μ g/ml aprotinin). Cells were scraped into a 1.5-ml microcentrifuge tube and gently rotated for 30 min at 4°C. After centrifugation (10,000 g for 30 min) the supernatant was collected as the NP-40-soluble fraction. The pellet was resuspended in 100 μ l of SDS-IP buffer (25 mM Hepes, pH 7.5, 4 mM EDTA, 25 mM NaF, 1% SDS, 1 mM Na₃VO₄) using Kontes homogenizers (Kontes, Vineland, NJ), and the homogenate was combined with 900 μ l of NP-40-IP buffer, which was used to wash the homogenizer. The lysate was passed 10 times through a 27G needle and then gently rotated again for 30 min at 4°C. After centrifugation (10,000 g for 30 min), the supernatant was used as the NP-40-insoluble fraction. The mixture of equal volume of NP-40-soluble and -insoluble fractions is called "total fraction."

For immunoprecipitation, 4 μ l of anti-occludin pAb (F5 or the mixture of F4 and F5) and a 15 μ l bed vol of rec-protein G-Sepharose 4B (Zymed Labs, Inc., South San Francisco, CA) were added to each fraction and rotated for 3 h at 4°C. Beads were washed five times with 1 ml of NP-40-IP buffer, from which immunoprecipitates were eluted by boiling in the SDS-PAGE sample buffer for 10 min. Samples were then separated by gel electrophoresis followed by immunoblotting or autoradiography.

Alkaline Phosphatase Treatment

After immunoprecipitation, beads were washed three times with 1 ml of NP-40-IP buffer and three times with 1 ml of AP buffer (50 mM Tris-HCl, pH 8.2, 50 mM NaCl, 1 mM MgCl₂, 1 mM dithiothreitol, 1 mM APMSF). They were then resuspended in 200 μ l of AP buffer containing 20 U of calf intestine alkaline phosphatase (Takara Shuzo Co., Ltd., Ohtsu, Japan). To check the specificity of the phosphatase, a phosphatase inhibitor (100 mM β -glycerophosphate, 25 mM NaF, 4 mM EDTA, 1 mM Na₃VO₄) was used. After a 1 h incubation at 30°C with occasional mixing, beads were washed three times with 1 ml of NP-40-IP buffer and boiled with SDS-PAGE sample buffer to elute the immunoprecipitates.

Gel Electrophoresis and Immunoblotting

Samples were resolved by one-dimensional SDS-PAGE as described by Laemmli (1970) and electrophoretically transferred to a nitrocellulose membrane (Protran, 0.45 μ m pore size; Schleicher & Schuell, Dassel, Germany). This membrane was incubated with primary antibodies, which were visualized using a blotting detection kit (Amersham Intl., Buckinghamshire, UK).

Metabolic Labeling and Phosphoamino Acid Analysis

Confluent monolayers of MDCK I cells were grown on filters, washed three times with phosphate-free MEM, and then incubated for 30 min in phosphate-free MEM containing 1% FCS dialyzed against 0.9% NaCl, 10 mM Hepes buffer (pH 7.4). Thereafter, [³²P]orthophosphate (Phosphorous-32; NEN Life Science Products, Boston, MA) was added at a concentration of 0.2 mCi/ml, cultured for 24 h, and then processed for immunoprecipitation.

Immunoprecipitates were resolved by gel electrophoresis and transferred to PVDF membranes (Immobilon; Millipore Corp., Bedford, MA), and signals were analyzed using a Fujix Bioimage Analyzer system (Bas 2000; Fuji Film Co. Ltd., Tokyo, Japan). Phosphoamino acids were analyzed based on the method of Boyle et al. (1991) with minor modifications. ³²P-labeled phosphorylated occludin bands in the NP-40-insoluble fraction were excised from membranes and hydrolyzed in 200 μ l of 6 M HCl at 110°C for 60 min. The hydrolysate was lyophilized using a speed vac concentrator (Savant Instruments Inc., Holbrook, NY) and resuspended in 10 μ l of pH 3.5 buffer (5% glacial acetic acid, 0.5% pyridine) containing cold phosphoamino acid standards. The sample was then spotted onto thin-layer cellulose plates (EM Science, Gibbstown, NJ), and two-dimen-

1. Abbreviations used in this paper: LC and NC, low and normal calcium; TER, transepithelial electric resistance.

sional electrophoresis was proceeded on a thin-layer system (NA-4000; Nippon Eido Co., Tokyo, Japan), using pH 3.5 buffer for the first dimension and pH 1.9 buffer (2.2% formic acid, 7.8% glacial acetic acid) for the second. The positions of ^{32}P -labeled phosphoamino acids were determined by autoradiography, and cold phosphoamino acid standards were visualized by ninhydrin staining.

Low Ca Medium Culture and Ca Switch

Confluent monolayers of MDCK I cells were grown in normal calcium (NC) medium (MEM with 5% FCS and 1.8 mM CaCl_2), washed three times with PBS, and then transferred to the low calcium (LC) medium (S-MEM [calcium-free MEM] supplemented with 5 μM CaCl_2 and 5% FCS that had been pretreated with Chelex resin [BioRad Labs., Inc., Hercules, CA]; Gumbiner et al., 1988). For the Ca switch, MDCK I cells in NC medium were trypsinized in PBS containing 1 mM EDTA, washed with PBS, and then plated on filters or cover slips in LC medium at a density of 2×10^5 cells/cm 2 . After a 36-h incubation in LC, cells were transferred to NC medium.

Immunofluorescence Microscopy

For indirect immunofluorescence microscopy, cells were cultured on cover slips and fixed in 1% formaldehyde in PBS for 15 min. After three washes with PBS they were permeabilized with 0.2% Triton X-100 in PBS for 15 min, soaked in blocking solution (PBS containing 1% BSA) for 15 min, and then incubated with first antibodies for 1 h in a moist chamber. The samples were washed three times with the blocking solution and then incubated for 30 min with the secondary antibodies, FITC-conjugated goat anti-rat IgG (Tago, Inc., Burlingame, CA) or rhodamine-conjugated goat anti-mouse IgG (Chemicon International, Inc., Temecula, CA). Samples were then washed with PBS three times, mounted in PBS containing 1% *p*-phenylenediamine and 90% glycerol, and examined using a fluorescence microscope (Zeiss Axiophot photomicroscope; Carl Zeiss, Inc., Thornwood, NY).

Chicken intestine was frozen in liquid nitrogen. About 7 μm -thick sections were cut in a cryostat, mounted on cover slips, and air dried. They were fixed in 95% ethanol at 4°C for 30 min and then in 100% acetone at room temperature for 1 min. After three washes with PBS, the sections were soaked in blocking solution for 15 min, incubated with primary antibodies for 60 min, washed three times with blocking solution containing 0.1% Triton X-100, and then incubated with secondary antibodies for 30 min. The samples were washed with PBS three times, mounted in PBS containing 1% *p*-phenylenediamine and 90% glycerol, and examined using a fluorescence microscope (Zeiss Axiophot photomicroscope; Carl Zeiss, Inc.) or a confocal fluorescence microscope (MRC 1024; BioRad Labs., Inc.) equipped with the photomicroscope.

Isolation of Junctional Fraction from Chick Liver

The junctional fraction was prepared from the liver of newly hatched or 1-d-old chicks through the crude membrane and the bile canaliculi fractions according to the method described previously (Tsukita and Tsukita, 1989; Furuse et al., 1993). The isolated junctional fraction was treated with SDS-IP buffer and processed for immunoprecipitation as described above.

Results

Multiple Banding and Detergent Solubility of Occludin

When the chicken junctional fraction isolated from liver and the whole cell lysate from cultured MDCK I cells were resolved by electrophoresis and immunoblotted with the respective anti-occludin Abs, both chicken and dog occludin migrated as multiple bands (Fig. 1 A). The apparent M_r of occludin in the confluent culture of MDCK I cells was distributed from 62 and 82 kD, and two or three bands of the lowest M_r were predominant. This multiple banding of occludin was found in all species so far examined.

As a first step to physiologically explain the multiple banding of occludin, we divided occludin from cultured MDCK I cells into NP-40-soluble and -insoluble fractions.

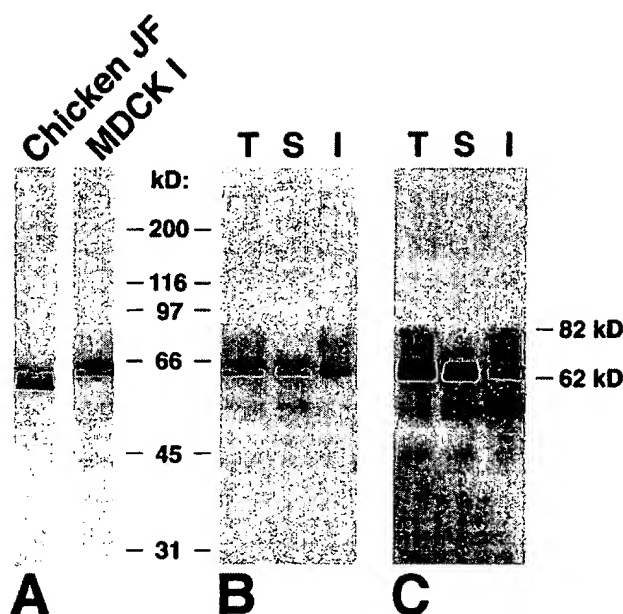


Figure 1. Multiple banding pattern and detergent solubility of occludin. (A) Immunoblots of the isolated junctional fraction from the chick liver (*Chicken JF*) and the whole cell lysate of MDCK I cells (*MDCK I*) with anti-chicken occludin mAb (Oc-2) and anti-mouse occludin pAb (F4), respectively. The apparent molecular masses of chicken and dog occludin were distributed between 58 and 66 kD and 62 and 82 kD, respectively. (B) Anti-occludin pAb (F4) immunoblots of the total (T), NP-40-soluble (S), and NP-40-insoluble (I) fractions of confluent MDCK I cells (see Materials and Methods). (C) Anti-occludin mAb (MOC37) immunoblots of the anti-occludin pAb (F4 + F5) immunoprecipitates from the total (T), NP-40-soluble (S), and NP-40-insoluble (I) fractions of confluent MDCK I cells. Since the amount of occludin in each fraction was fairly small (B), both NP-40-soluble and -insoluble occludins were recovered by immunoprecipitation, electrophoresed, and immunoblotted (C). Comparison between B and C revealed that the efficiency of immunoprecipitation from NP-40-soluble fraction is almost the same as that from NP-40-insoluble fraction. Higher M_r bands of occludin were selectively recovered in the NP-40-insoluble fraction.

Confluent cultures of MDCK I cells, which were grown on filters and showed $>2,000 \Omega\text{cm}^2$ of TER, were solubilized with 1% NP-40, and the supernatant was used as the NP-40-soluble fraction. The pellet was further solubilized with lysis buffer containing 1% SDS, which was then used as the NP-40-insoluble fraction. Occludin was almost undetectable in the SDS-insoluble sediment by immunoblotting. Since the amount of occludin in each fraction was fairly small (Fig. 1 B), both NP-40-soluble and -insoluble occludins were recovered by immunoprecipitation with anti-occludin pAb, electrophoresed, and immunoblotted with anti-occludin mAb. Fig. 1 C shows that under the NP-40 extraction conditions used in this study, the predominant lower M_r two or three bands of occludin were mostly recovered in the NP-40-soluble fraction, and the higher M_r bands were partitioned into the NP-40-insoluble fraction. The same result was obtained when mouse and human cultured epithelial cells, MTD-1A and T84 cells, respectively, were used (data not shown).

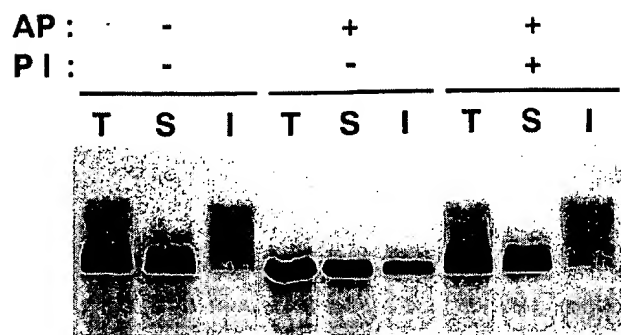


Figure 2. Alkaline phosphatase treatment. Anti-occludin pAb (F4 + F5) immunoprecipitates from the total (T), NP-40-soluble (S), and NP-40-insoluble (I) fractions of confluent MDCK I cells were incubated in the presence (+) or absence (-) of alkaline phosphatase (AP) and its specific inhibitor (PI) and then immunoblotted with anti-occludin mAb (MOC37). Alkaline phosphatase significantly decreased the apparent molecular masses of NP-40-soluble and -insoluble occludin bands to the level of the lowest M_r band, and its inhibitor completely suppressed this effect.

Electrophoretic Mobility and Phosphorylation Level of Occludin

It is likely that some posttranslational modification causes the multiple banding of occludin. We first determined whether or not phosphorylation increases apparent M_r of occludin in SDS-PAGE. The immunoprecipitated occludin from NP-40-soluble and -insoluble fractions were then

treated with alkaline phosphatase (Fig. 2). This procedure significantly decreased the apparent M_r of NP-40-soluble and -insoluble occludin bands to the level of the lowest M_r band. This activity of alkaline phosphatase was completely suppressed by its inhibitor, indicating that phosphorylation causes the upward shift of occludin band in SDS-PAGE.

To determine which types of amino acid residues are phosphorylated, we analyzed phosphoamino acids using cultured MDCK I cells that were metabolically labeled with [32 P] orthophosphate. Both NP-40-soluble and -insoluble occludins were labeled, although the latter were phosphorylated more heavily in terms of specific activity than the former (Fig. 3 A). Within the insoluble occludin, the specific activity was considerably higher in the higher M_r bands than the lower M_r bands (Fig. 3 B). The [32 P]phosphoamino acids were then released by partial acid hydrolysis of the 32 P-labeled higher M_r bands of NP-40-insoluble occludin as well as the 32 P-labeled NP-40-soluble occludin, and identified by thin-layer electrophoresis. As shown in Fig. 3 C, in NP-40-soluble occludin, both serine and threonine residues were phosphorylated whereas in higher M_r bands of NP-40-insoluble occludin, serine residues were predominantly phosphorylated with slight threonine phosphorylation. Phospho-tyrosine was undetectable either in NP-40-soluble or -insoluble occludin.

Behavior of Occludin during Destruction and Formation of Tight Junctions

We examined the relationship between NP-40-insoluble occludin and tight junction formation. First, the banding pat-

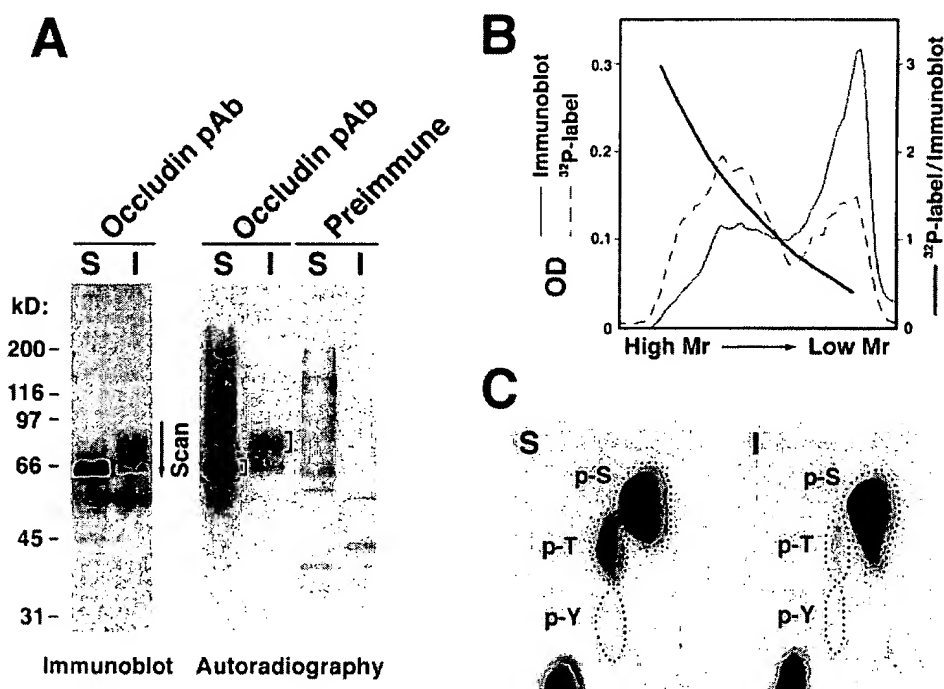


Figure 3. Phosphoamino acid analysis of the NP-40-soluble and -insoluble occludin. (A) Anti-occludin mAb (MOC37) immunoblots (Immunoblot) and accompanying autoradiograms (Autoradiography) of anti-occludin pAb (F5) immunoprecipitates from the NP-40-soluble (S) and NP-40-insoluble (I) fractions of confluent MDCK I cells metabolically labeled with [32 P] orthophosphate. Control experiments were performed using preimmune serum (Pre-immune). (B) Relative specific activity of occludin bands. The region marked by an arrow in the immunoblot and autoradiogram lanes of NP-40-insoluble occludin was scanned by densitometry (A, Scan). Relative specific activity of each occludin band was calculated as autoradiogram density/immunoblot density. (C) The marked region in the

autoradiogram lane of 32 P-labeled NP-40-soluble and -insoluble occludins was excised and processed for phosphoamino acid analysis. The positions of phosphoserine (p-S), phosphothreonine (p-T), and phosphotyrosine (p-Y) were determined by autoradiography through comparison with the ninhydrin staining profiles of unlabeled phosphoamino acid standards. In NP-40-soluble occludin, both serine and threonine residues were phosphorylated (S), whereas in higher M_r bands of NP-40-insoluble occludin, serine residues were predominantly phosphorylated with slight phosphorylation of threonine residues (I).

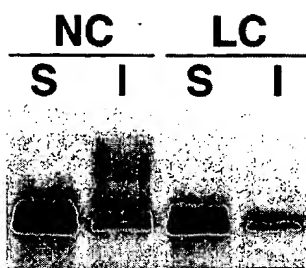


Figure 4. Multiple banding pattern and detergent solubility of occludin in MDCK I cells grown in normal calcium (1.8 mM; NC) or low calcium (5 μ M; LC) medium for 24 h. Anti-occludin pAb (F4 + F5) immunoprecipitates from the NP-40-soluble (S) and NP-40-insoluble (I) fractions of confluent MDCK I cells were immunoblotted

with anti-occludin mAb (MOC37). Under low calcium conditions, the amount of NP-40-insoluble occludin was fairly small.

terns of NP-40-soluble and -insoluble occludin of MDCK I cells were compared under conditions of normal (1.8 mM) and low (5 μ M) calcium medium. Fig. 4 shows that under low calcium (LC) conditions, almost all occludin was solubilized by 1% NP-40 and migrated as two or three lower M_r bands in SDS-PAGE, whereas the insoluble fraction was fairly small. Furthermore, the total amount of occludin was significantly decreased under LC conditions. We then transferred cells from the LC to the normal calcium (NC) medium (Fig. 5). Within 10 min the amount of occludin recovered as the NP-40-insoluble fraction was significantly increased, followed by a gradual increase of their apparent M_r . No significant change of either the banding pattern or the amount of the NP-40-soluble occludin was detected after the Ca switch. The same results were obtained also from confluent cultures of mouse (MTD-1A) and human (T84) epithelial cells (data not shown).

The behavior of occludin as well as ZO-1 during the formation of tight junctions initiated by the Ca switch was then examined by immunofluorescence microscopy using confluent MDCK I cells (Fig. 6). In the LC medium, occludin signal was detected mainly from small granular structures scattered in the cytoplasm, and ZO-1 was found on ring-like structures that may consist of actin filament bundles. Some large granular structures and some ring-like structures were occasionally occludin/ZO-1 double positive. Within 10 min after the cells were transferred to the NC medium, both occludin and ZO-1 started to accumulate and colocalize at the cell-cell borders as discontinuous lines. Around 60 min after the Ca switch, this accumulation process appeared to reach a plateau, resulting in the continuous linear concentration of occludin and ZO-1 at junctional regions.

A Monoclonal Antibody Specific for Phosphorylated Type of Occludin

In the previous study we obtained three mAbs that recognized distinct epitopes of chicken occludin: Oc-1, Oc-2, and Oc-3 (Furuse et al., 1993). When the isolated junctional fraction from chick liver was immunoblotted with these mAbs, the banding pattern obtained from Oc-3 differed from those with Oc-1 and Oc-2 (Fig. 7; see Fig. 1 in Furuse et al., 1993). Oc-3 did not recognize the predominant lower M_r bands of occludin, which were clearly detected by Oc-1 and Oc-2. This suggests that Oc-3 is specific for phosphorylated occludin. To evaluate this notion, chicken occludin in the isolated junctional fraction was solubilized

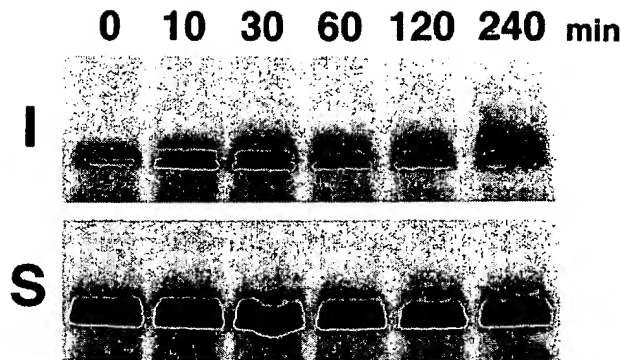


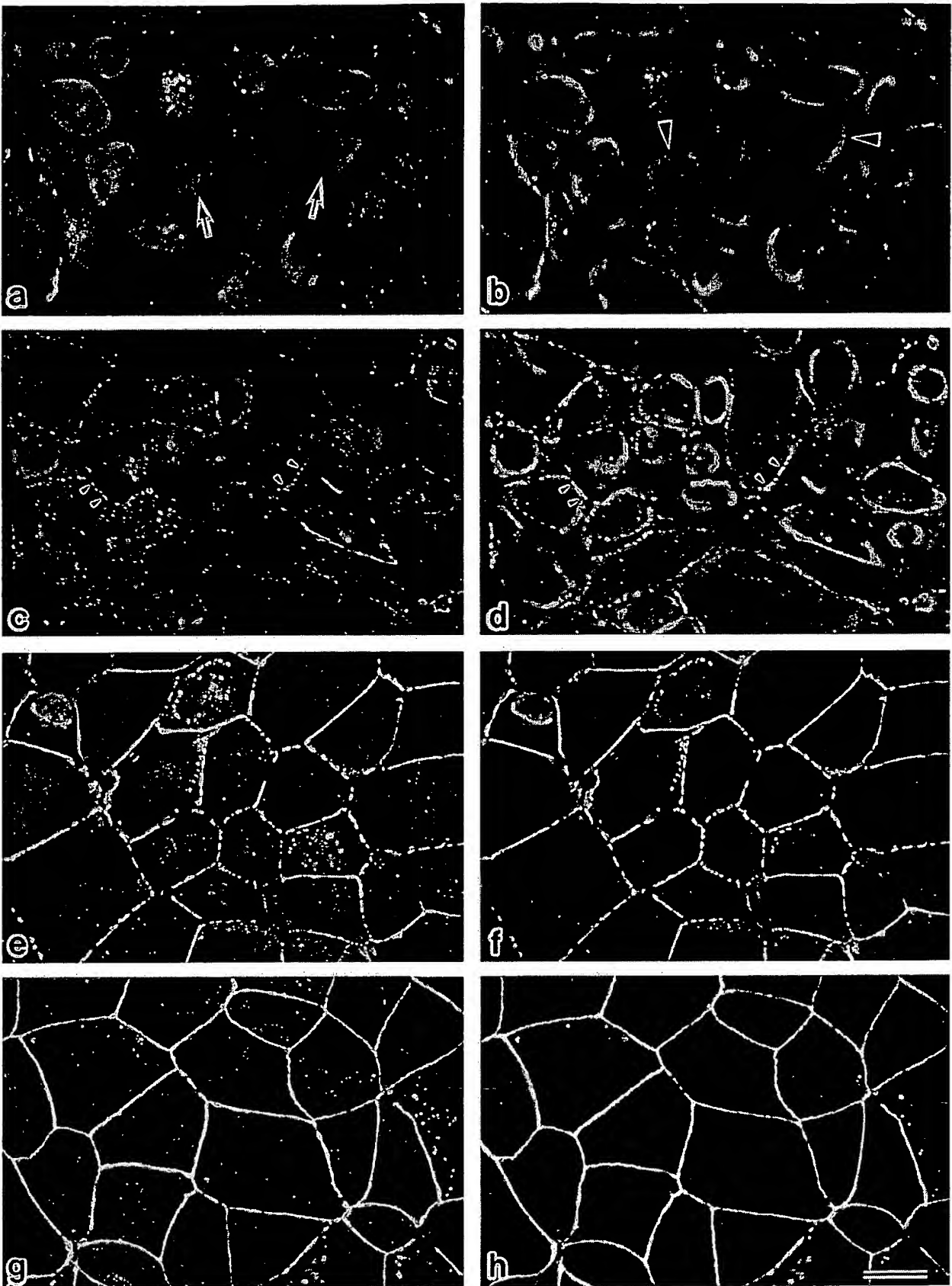
Figure 5. Insolubilization and upward band shift of occludin in MDCK I cells after switching from low (5 μ M) to normal (1.8 mM) calcium medium. 0, 10, 30, 60, 120, and 240 min after the Ca switch, the anti-occludin pAb (F4 + F5) immunoprecipitates from the NP-40-insoluble (I) or NP-40-soluble (S) fractions of confluent MDCK I cells were immunoblotted with anti-occludin mAb (MOC37). Within 10 min after switching, the amount of occludin recovered as the NP-40-insoluble portion was significantly increased, followed by a gradual increase of their apparent molecular masses.

using 1% SDS, immunoprecipitated with anti-chicken occludin pAb, treated with alkaline phosphatase in the absence or presence of its specific inhibitor, and then immunoblotted with Oc-2 or Oc-3 (Fig. 7). Immunoblots of chicken occludin with Oc-2 showed that alkaline phosphatase converged the multiple bands into the lowest M_r of 58 kD, which was suppressed by the phosphatase inhibitor. Oc-2 detected this dephosphorylated occludin, whereas Oc-3 hardly recognized it. We concluded that Oc-3 is specific for the phosphorylated type.

Since Oc-2 or Oc-3 does not recognize mammalian occludin (Furuse et al., 1993), we examined the subcellular distribution of the phosphorylated occludin in chicken tissues using Oc-3 and compared it with the Oc-2 staining, which represents the distribution of total occludin. As shown in Fig. 8, Oc-2 stained the junctional complex regions of intestinal epithelial cells in a linear fashion. In addition, the basolateral membrane domains and the cytoplasm of these cells was also stained in a dotted manner. By contrast, Oc-3 mainly stained tight junction proper, showing a very weak signal only from the basolateral membrane domains. These observations indicate that the highly phosphorylated form of occludin is selectively concentrated at the tight junction proper.

Discussion

Occludin has been characterized in various species by its multiple bands on SDS-PAGE (Furuse et al., 1993; Saitou et al., 1997). The present study showed that occludin is phosphorylated at serine and threonine residues, which shifts the occludin band to assume the multiple profile in SDS-PAGE. Canine occludin is detected as at least 10 closely migrating bands between 62 and 82 kD. This suggests that several serine and threonine residues can be phosphorylated per occludin molecule and that the degree of the upward band shift of occludin roughly parallels its



AP : - + + - + +
 PI : - - + - - +

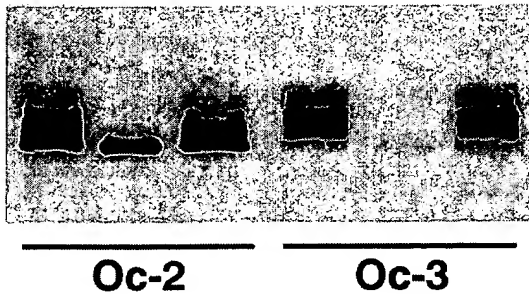


Figure 7. Two distinct anti-chicken occludin mAbs, Oc-2 and Oc-3. Chicken occludin in the isolated junctional fraction was solubilized using 1% SDS, immunoprecipitated with anti-chicken occludin pAb (F44), incubated in the presence (+) or absence (-) of alkaline phosphatase (AP) and its inhibitor (PI), and then immunoblotted with Oc-2 or -3. Oc-3 could not detect dephosphorylated occludin, whereas Oc-2 recognized both phosphorylated and dephosphorylated occludin.

phosphorylation level. Phosphoamino acid analyses of higher and lower M_r bands of occludin suggested that threonine residues are phosphorylated followed by heavy serine phosphorylation during the upward shift of occludin bands. However, it remains elusive whether these serine/threonine residues are phosphorylated sequentially or randomly in each molecule and whether or not the phosphorylation of some residues is functionally more important than that of others.

Highly phosphorylated occludin from confluent cultures of MDCK I cells resisted extraction with 1% NP-40. Judging from the alkaline phosphatase treatment, not only the nonphosphorylated but also the less phosphorylated form of occludin was solubilized with 1% NP-40. Although the optimal concentration of NP-40 used here was empirically determined as 1%, it can be concluded that the highly phosphorylated type of occludin is more resistant to detergent extraction than the less phosphorylated type. When MDCK I cells were cultured in the LC medium, tight junctions disappeared, most occludin became soluble with 1% NP-40, and highly phosphorylated occludin was hardly detected. The total amount of occludin appeared to be decreased, suggesting the up-regulated degradation and/or down-regulated de novo synthesis of occludin under LC conditions. When these cells were transferred to the NC medium, tight junctions began to be assembled. With a similar time course, the amount of NP-40-insoluble occludin markedly increased, followed by a gradual upward

shift of bands. Considering that tight junction strands are resistant to detergent extraction (Stevenson and Goodenough, 1984; Stevenson et al., 1988), these findings suggested that highly phosphorylated occludin predominantly composes the tight junction proper. This conclusion was confirmed by the immunofluorescence analyses of chicken epithelial cells using the mAb Oc-3, which is specific for phosphorylated occludin.

Occludin is at least one of the major components of tight junction strands *in situ* (Furuse et al., 1993; Fujimoto et al., 1995; Saitou et al., 1997). Furthermore, judging from occludin overexpression studies using insect Sf9 cells, occludin by itself may form tight junction strand-like structures, probably through oligomerization (Furuse et al., 1996). On the other hand, occludin binds to ZO-1 (then to cytoskeletons) at its COOH-terminal ~150 amino acid region. Therefore, at present there are at least two possible molecular mechanisms by which occludin can become resistant to NP-40 extraction: oligomerization and cytoskeleton association. Further analyses are required to evaluate these two possibilities.

Understanding of the behavior of occludin during tight junction formation is still limited compared to that of adhesion molecules in other intercellular junctions. For example, in epithelial cells, cadherins are reportedly associated with β catenin in the endoplasmic reticulum, appear on the basolateral membrane surface as cadherin- $\alpha\beta$ catenin complexes, and laterally aggregate (or oligomerize) at the most apical part of the lateral membrane to form adherens junctions (Hinck et al., 1994; Näthke et al., 1994). As for tight junction formation, the following questions should be addressed. Where does occludin associate with ZO-1 and other tight junction-associated peripheral membrane proteins? Where are occludin molecules oligomerized? Is occludin (or occludin-peripheral membrane proteins complex) targeted to the basolateral membranes or directly to the junctional complex area? Introduced exogenous chicken occludin reportedly concentrates in cytoplasmic vesicular structures in MDCK I cells, when the transfectants are cultured in LC medium (McCarthy et al., 1996). As shown here, endogenous occludin is also distributed in cytoplasmic granular structures under LC conditions, and most of them do not colocalize with ZO-1. Although the Ca switch appears to recruit these cytoplasmic occludins, together with ZO-1, to the cell-cell contact regions, at present it is difficult to exclude the possibility that some or all of the cytoplasmic occludin-positive granular structures occur as a result of endocytosis under LC conditions. The difference between the Oc-2 and -3 staining patterns in chicken epithelial cells suggests that non- or less phosphorylated occludin is first targeted to the basolateral membranes from the cytoplasm and that further phosphorylation induces occludin to concentrate into the junctional complex region.

Figure 6. Formation of tight junctions in MDCK I cells after a Ca switch from low (5 μ M) to normal (1.8 mM) calcium medium. 0 (a and b), 10 (c and d), 30 (e and f), and 60 (g and h) min after the Ca switch, confluent MDCK I cells were fixed and immunofluorescently stained with rat anti-occludin mAb (a, c, e, and g) and mouse anti-ZO-1 mAb (b, d, f, and h). In the low calcium medium (a and b), occludin signal was detected mainly from small granular structures in the cytoplasm (arrows), and ZO-1 signal was from ring-like structures (arrowheads). Within 10 min after the Ca switch (c and d), both occludin and ZO-1 gradually began to accumulate and colocalize at cell-cell borders (arrowheads). 30–60 min after the Ca switch (e–h), both occludin and ZO-1 were colocalized in a linear fashion at junctional regions. Even 60 min after the Ca switch, the epithelial sheet was still leaky in terms of TER. Bar, 20 μ m.

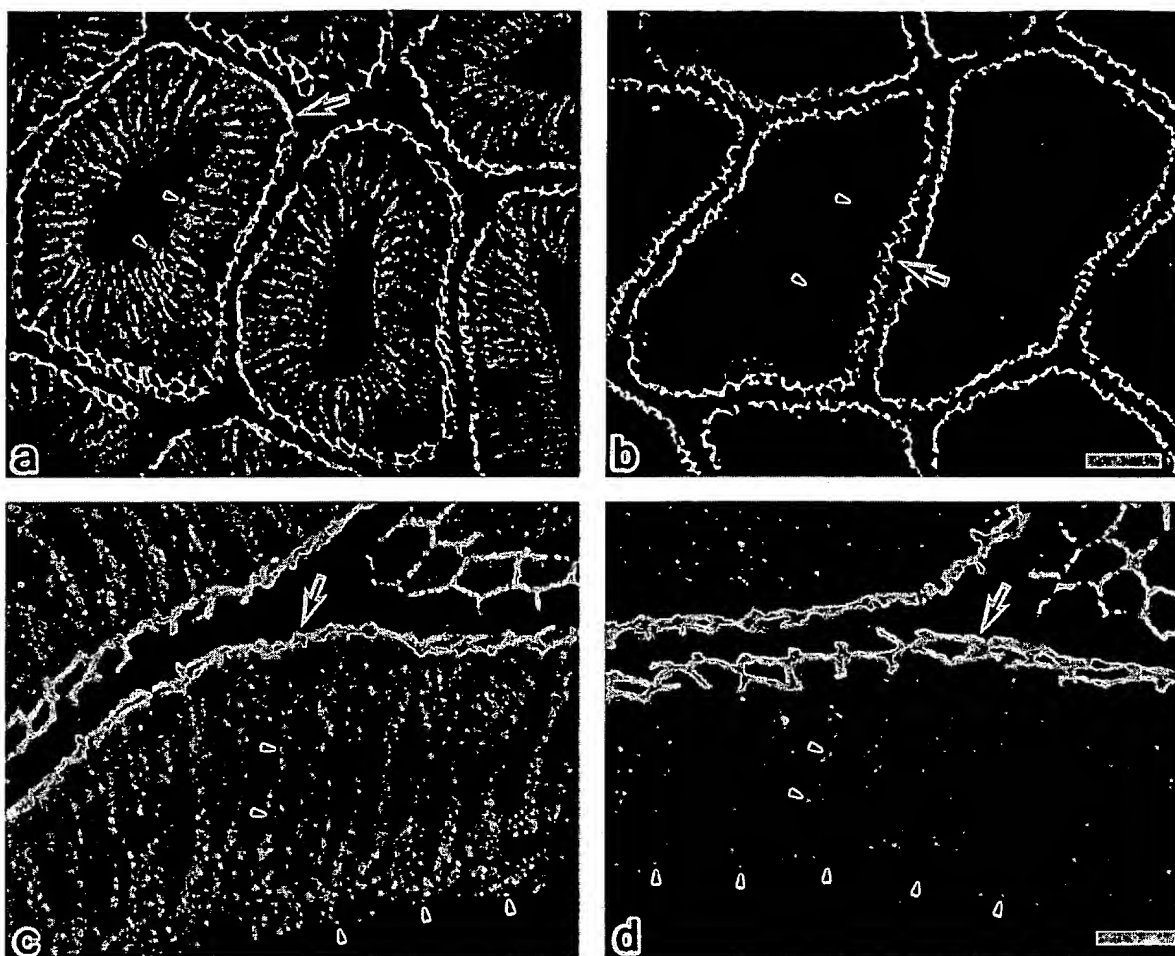


Figure 8. Confocal immunofluorescence microscopy of frozen sections of chick intestinal epithelial cells with anti-chicken occludin mAb, Oc-2 (*a* and *c*), or Oc-3 (*b* and *d*). Oc-2 stained both the junctional complex regions (*arrows*) and the basolateral membrane domains (*arrowheads*) in linear and dotted manners, respectively. By contrast, Oc-3 mainly stained the tight junction region (*arrows*), showing a very weak signal only from the basolateral membranes (*arrowheads*). In our previous study (Furuse et al., 1993) it was emphasized that Oc-2 is specific for tight junctions without paying special attention to its staining at the basolateral membrane domains, but as shown here, the difference in the staining pattern is significant between Oc-2 and -3. Bars: (*a* and *b*) 30 μ m; (*c* and *d*) 10 μ m.

Another issue that should be discussed is the similarity between occludin and connexin in terms of phosphorylation as well as structure. Connexin is an integral channel protein functioning at gap junctions (Bruzzone et al., 1996; Kumar and Gilula, 1996). Connexin also bears four transmembrane domains, although there is no sequence similarity between connexin and occludin (Furuse et al., 1993; Ando-Akatsuka et al., 1996). Connexin43 is reportedly serine phosphorylated in gap junction communication-competent cells (Musil et al., 1990). This phosphorylation mostly occurs after the arrival of non- or slightly phosphorylated connexin43 at the plasma membrane (Musil and Goodenough, 1991; Laird et al., 1995). The strong correlation between the formation of functional gap junctions and the phosphorylation of connexin is very similar to that between the formation of tight junctions and the phosphorylation of occludin.

Studies using various protein kinase activators and inhibitors have revealed that protein phosphorylation, especially the protein kinase C-dependent type, plays an im-

portant role in tight junction assembly and functions (Balda et al., 1991, 1993; Citi, 1992; Denisenko et al., 1994; Citi and Denisenko, 1995; Stuart and Nigam, 1995). However, a positive correlation has not been obtained between the tight junction assembly and the phosphorylation level of tight junction proteins such as ZO-1 and -2, p130, and cingulin (Balda et al., 1993; Citi and Denisenko, 1995). We found here, however, that occludin is heavily serine/threonine phosphorylated in a similar time course as that of tight junction formation after a Ca switch, and that the highly phosphorylated occludin is selectively concentrated at tight junctions. This suggests that protein phosphorylation is directly involved in tight junction assembly and provides a new experimental approach to studying the molecular mechanism of the regulation of tight junction assembly. In our next step we should determine which serine/threonine residues of occludin are phosphorylated *in vivo*, which kinases phosphorylate these residues, whether mutations at these residues affect the tight junction assembly and function, and which signaling up or

down regulates occludin phosphorylation. Studies along these lines will clarify in molecular terms, how the barrier and fence functions of tight junctions are regulated in vivo.

We would like to thank all the members of our laboratory (Department of Cell Biology, Kyoto University Faculty of Medicine) for helpful discussions throughout this study. Our thanks are also due to Drs. T. Moriguchi and E. Nishida (Department of Genetics and Molecular Biology, Institute for Virus Research, Kyoto University) for technical help with the phosphoamino acid analysis.

This work was supported in part by a Grant-in-Aid for Cancer Research and a Grant-in-Aid for Scientific Research (A) from the Ministry of Education, Science and Culture of Japan to S. Tsukita.

Received for publication 16 January 1997 and in revised form 14 March 1997.

References

- Anderson, J.M., B.R. Stevenson, L.A. Jesaitis, D.A. Goodenough, and M.S. Mooseker. 1988. Characterization of ZO-1, a protein component of the tight junction from mouse liver and Madin-Darby canine kidney cells. *J. Cell Biol.* 106:1141-1149.
- Ando-Akatsuka, Y., M. Saitou, T. Hirase, M. Kishi, A. Sakakibara, M. Itoh, S. Yonemura, M. Furuse, and Sh. Tsukita. 1996. Interspecies diversity of the occludin sequence: cDNA cloning of human, mouse, dog, and rat-kangaroo homologues. *J. Cell Biol.* 133:43-47.
- Balda, M.S., L. Gonzalez-Mariscal, R.G. Contreras, M. Macias-Silva, M.E. Torres-Marquez, J.A. Garcia-Sainz, and M. Cerejido. 1991. Assembly and sealing of tight junctions: possible participation of G-proteins, phospholipase C, protein kinase C and calmodulin. *J. Membr. Biol.* 122:193-202.
- Balda, M.S., L. Gonzalez-Mariscal, K. Matter, M. Cerejido, and J.M. Anderson. 1993. Assembly of the tight junction: the role of diacylglycerol. *J. Cell Biol.* 123:293-302.
- Balda, M.S., J.A. Whitney, C. Flores, S. González, M. Cerejido, and K. Matter. 1996. Functional dissociation of paracellular permeability and transepithelial electrical resistance and disruption of the apical-basolateral intramembrane diffusion barrier by expression of a mutant tight junction membrane protein. *J. Cell Biol.* 134:1031-1049.
- Boyle, W.J., P. van der Geer, and T. Hunter. 1991. Phosphopeptide mapping and phosphoamino acid analysis by two-dimensional separation on thin-layer cellulose plates. *Methods Enzymol.* 201:110-148.
- Bruzzone, R., T.W. White, and D.A. Goodenough. 1996. The cellular internet: on-line with connexins. *Bioessays.* 18:709-718.
- Citi, S. 1992. Protein kinase inhibitors prevent junction dissociation induced by low extracellular calcium in MDCK epithelial cells. *J. Cell Biol.* 117:169-178.
- Citi, S. 1993. The molecular organization of tight junctions. *J. Cell Biol.* 121:485-489.
- Citi, S., and N. Denisenko. 1995. Phosphorylation of the tight junction protein cingulin and the effects of protein kinase inhibitors and activators in MDCK epithelial cells. *J. Cell Sci.* 108:2917-2926.
- Citi, S., H. Sabanay, R. Jakes, B. Geiger, and J. Kendrick-Jones. 1988. Cingulin, a new peripheral component of tight junctions. *Nature (Lond.)* 33:272-276.
- Denisenko, N., P. Burighel, and S. Citi. 1994. Different effects of protein kinase inhibitors on the localization of junctional proteins at cell-cell contact sites. *J. Cell Sci.* 107:969-981.
- Farquhar, M.G., and G.E. Palade. 1963. Junctional complexes in various epithelia. *J. Cell Biol.* 17:375-409.
- Fujimoto, K. 1995. Freeze-fracture replica electron microscopy combined with SDS digestion for cytochemical labeling of integral membrane proteins. Application to the immunogold labeling of intercellular junctional complexes. *J. Cell Sci.* 108:3443-3449.
- Furuse, M., T. Hirase, M. Itoh, A. Nagafuchi, S. Yonemura, Sa. Tsukita, and Sh. Tsukita. 1993. Occludin: a novel integral membrane protein localizing at tight junctions. *J. Cell Biol.* 123:1777-1788.
- Furuse, M., M. Itoh, T. Hirase, A. Nagafuchi, S. Yonemura, Sa. Tsukita, and Sh. Tsukita. 1994. Direct association of occludin with ZO-1 and its possible involvement in the localization of occludin at tight junctions. *J. Cell Biol.* 127:1617-1626.
- Furuse, M., K. Fujimoto, N. Sato, T. Hirase, Sa. Tsukita, and Sh. Tsukita. 1996. Overexpression of occludin, a tight junction-associated integral membrane protein, induces the formation of intracellular multilamellar bodies bearing tight junction-like structures. 109:429-435.
- Gumbiner, B. 1987. Structure, biochemistry, and assembly of epithelial tight junctions. *Am. J. Physiol.* 253:C749-C758.
- Gumbiner, B. 1993. Breaking through the tight junction barrier. *J. Cell Biol.* 123:1631-1633.
- Gumbiner, B., B. Stevenson, and A. Grimaldi. 1988. The role of the cell adhesion molecule uvomorlin in the formation and maintenance of the epithelial junctional complex. *J. Cell Biol.* 107:1575-1587.
- Gumbiner, B., T. Lowenkopf, and D. Apatira. 1991. Identification of a 160kDa polypeptide that binds to the tight junction protein ZO-1. *Proc. Natl. Acad. Sci. USA.* 88:3460-3464.
- Hinck, L., I.S. Näthke, J. Papkoff, and W.J. Nelson. 1994. Dynamics of cadherin/catenin complex formation: novel protein interactions and pathways of complex assembly. *J. Cell Biol.* 125:1327-1340.
- Itoh, M., S. Yonemura, A. Nagafuchi, Sa. Tsukita, and Sh. Tsukita. 1991. A220-kD undercoat-constitutive protein: Its specific localization at cadherin-based cell-cell adhesion sites. *J. Cell Biol.* 115:1449-1462.
- Itoh, M., A. Nagafuchi, S. Yonemura, T. Kitani-Yasuda, Sa. Tsukita, and Sh. Tsukita. 1993. The 220-kD protein colocalizing with cadherins in non-epithelial cells is identical to ZO-1, a tight junction-associated protein in epithelial cells: cDNA cloning and immunoelectron microscopy. *J. Cell Biol.* 121:491-502.
- Jesaitis, L.A., and D.A. Goodenough. 1994. Molecular characterization and tissue distribution of ZO-2, a tight junction protein homologous to ZO-1 and the *Drosophila* discs-large tumor suppressor protein. *J. Cell Biol.* 124:949-961.
- Keon, B.H., S. Schäfer, C. Kuhn, C. Grund, and W.W. Franke. 1996. Symplekin, a novel type of tight junction plaque protein. *J. Cell Biol.* 134:1003-1018.
- Kumar, N.M., and N.B. Gilula. 1996. The gap junction communication channel. *Cell.* 84:381-388.
- Laemmli, U.K. 1970. Cleavage of structural proteins during the assembly of the head of bacteriophage T4. *Nature (Lond.)* 227:680-685.
- Laird, D.W., M. Castillo, and L. Kasprzak. 1995. Gap junction turnover, intracellular trafficking, and phosphorylation of connexin43 in brefeldin A-treated rat mammary tumor cells. *J. Cell Biol.* 131:1193-1203.
- Lum, H., and A.B. Malik. 1994. Regulation of vascular endothelial barrier function. *Am. J. Physiol.* 267:L223-L241.
- Madara, J.L. 1987. Intestinal absorptive cell tight junctions are linked to cytoskeleton. *Am. J. Physiol.* 253:C171-C175.
- Madara, J.L., and J.R. Pappenheimer. 1987. Structural basis for physiological regulation of paracellular pathways in intestinal epithelia. *J. Membr. Biol.* 100:149-164.
- McCarthy, K.M., I.B. Skare, M.C. Stankewich, M. Furuse, Sh. Tsukita, R.A. Rogers, R.D. Lynch, and E.E. Schneeberger. 1996. Occludin is a functional component of the tight junction. *J. Cell Sci.* 109:2287-2298.
- Musil, L.S., and D.A. Goodenough. 1991. Biochemical analysis of connexin43 intracellular transport, phosphorylation, and assembly into gap junctional plaques. *J. Cell Biol.* 115:1357-1374.
- Musil, L.S., B.A. Cunningham, G.M. Edelman, and D.A. Goodenough. 1990. Differential phosphorylation of the gap junction protein connexin43 in junctional communication-competent and -deficient cell lines. *J. Cell Biol.* 111:2077-2088.
- Näthke, I.S., L. Hinck, J.R. Swedlow, J. Papkoff, and W.J. Nelson. 1994. Defining interactions and distribution of cadherin and catenin complexes in polarized epithelial cells. *J. Cell Biol.* 125:1341-1352.
- Saitou, M., Y. Ando-Akatsuka, M. Itoh, M. Furuse, J. Inazawa, K. Fujimoto, and Sh. Tsukita. 1997. Mammalian occludin in epithelial cells: Its expression and subcellular distribution. *Eur. J. Cell Biol.* In press.
- Schneeberger, E.E., and R.D. Lynch. 1992. Structure, function, and regulation of cellular tight junctions. *Am. J. Physiol.* 262:L647-L661.
- Stevenson, B.R., and D. Goodenough. 1984. Zonula occludens in junctional complex-enriched fractions from mouse liver: preliminary morphological and biochemical characterization. *J. Cell Biol.* 98:1209-1221.
- Stevenson, B.R., J.D. Siliciano, M.S. Mooseker, and D.A. Goodenough. 1986. Identification of ZO-1: a high molecular weight polypeptide associated with the tight junction (zonula occludens) in a variety of epithelia. *J. Cell Biol.* 103:755-766.
- Stevenson, B.R., J.M. Anderson, and S. Bullivant. 1988. The epithelial tight junction: Structure, function and preliminary biochemical characterization. *Mol. Cell Biochem.* 83:129-145.
- Stuart, R.O., and S.K. Nigam. 1995. Regulated assembly of tight junctions by protein kinase C. *Proc. Natl. Acad. Sci. USA.* 92:6072-6076.
- Tsukita, Sh., and Sa. Tsukita. 1989. Isolation of cell-to-cell adherens junctions from rat liver. *J. Cell Biol.* 108:31-41.
- Willott, E., M.S. Balda, A.S. Fanning, B. Jameson, C. Van Itallie, and J.M. Anderson. 1993. The tight junction protein ZO-1 is homologous to the *Drosophila* discs-large tumor suppressor protein of septate junctions. *Proc. Natl. Acad. Sci. USA.* 90:7834-7838.
- Wong, V., and B.M. Gumbiner. 1997. A synthetic peptide corresponding to the extracellular domain of occludin perturbs the tight junction permeability barrier. *J. Cell Biol.* 136:399-409.
- Zhong, Y., T. Saitoh, T. Minase, N. Sawada, K. Enomoto, and M. Mori. 1993. Monoclonal antibody 7H6 reacts with a novel tight junction-associated protein distinct from ZO-1, cingulin, and ZO-2. *J. Cell Biol.* 120:477-483.

The junction-associated protein, zonula occludens-1, localizes to the nucleus before the maturation and during the remodeling of cell–cell contacts

(tight junctions/intercellular junctions/membrane-associated guanylate kinase homologues/wound healing)

CARA J. GOTTARDI*[†], MONIQUE ARPIN*, ALAN S. FANNING[‡], AND DANIEL LOUVARD*

*Laboratory of Cell Signaling and Morphogenesis, UMR 144 Centre National de la Recherche Scientifique, Institut Curie 75231 Paris Cedex 05, France; and

[‡]Department of Internal Medicine, Yale University School of Medicine, New Haven, CT 06510

Communicated by David D. Sabatini, New York University Medical Center, New York, NY, July 15, 1996 (received for review April 8, 1996)

ABSTRACT The junction-associated protein zonula occludens-1 (ZO-1) is a member of a family of membrane-associated guanylate kinase homologues thought to be important in signal transduction at sites of cell–cell contact. We present evidence that under certain conditions of cell growth, ZO-1 can be detected in the nucleus. Two different antibodies against distinct portions of the ZO-1 polypeptide reveal nuclear staining in subconfluent, but not confluent, cell cultures. An exogenously expressed, epitope-tagged ZO-1 can also be detected in the nuclei of transfected cells. Nuclear accumulation can be stimulated at sites of wounding in cultured epithelial cells, and immunoperoxidase detection of ZO-1 in tissue sections of intestinal epithelial cells reveals nuclear labeling only along the outer tip of the villus. These results suggest that the nuclear localization of ZO-1 is inversely related to the extent and/or maturity of cell contact. Since cell–cell contacts are specialized sites for signaling pathways implicated in growth and differentiation, we suggest that the nuclear accumulation of ZO-1 may be relevant for its suggested role in membrane-associated guanylate kinase homologue signal transduction.

Zonula occludens-1 (ZO-1) is a 210- to 225-kDa peripheral membrane protein of unknown function. It is found associated with the cytoplasmic surfaces of tight junctions (1, 2), cell–cell contacts of cultured nonepithelial brain astrocytes (3), and the intercalated disks (a modified adherens junction) of cardiac myocytes (4). Localization to these structures seems to require established cell–cell contacts, since treatments that prevent the homotypic interaction of E-cadherins (5, 6) or block downstream signaling from this interaction (7) inhibit recruitment of ZO-1 to the margin of cell–cell contact.

ZO-1 has recently been identified as a member of a family of putative signaling proteins called membrane-associated guanylate kinase homologues (MAGUKs; ref. 8). The founding member of this family is the product of the lethal (1) discs-large-1 (*dlg*) tumor suppressor gene of *Drosophila* (9). Loss-of-function alleles of *dlg* affect junction formation and result in the overgrowth of imaginal wing disc epithelia, suggesting that this junction associated protein may play a role in epithelial growth control. Other members of this family include: ZO-2, a second tight junction-associated protein (10); PSD-95/SAP-90 and SAP-97, which localize to synaptic junctions (11, 12); p55, which participates in erythrocyte membrane-cytoskeletal interactions (13); the *lin 2* gene product of *Caenorhabditis elegans* (14); and a human homologue of *dlg*, *hdlg* (15).

MAGUK family members are generally associated with the plasma membrane and cytoskeletal elements at specialized

sites of cell–cell contact. They manifest a conserved modular organization of domains that show homology to functionally defined signaling molecules: a src homology region 3 (SH3 domain), a region homologous to guanylate kinases, and an 80- to 90-aa GLGF motif (termed PDZ domains, for PSD-95/Discs-large/ZO-1; originally described by M. Kennedy, California Institute of Technology, Pasadena, CA). Recent evidence suggests that PDZ domains mediate interactions with certain plasma membrane proteins and may enable MAGUKs to crosslink certain transmembrane proteins to the cortical cytoskeleton (16, 17). Moreover, ZO-1 uniquely contains a region of proline-rich stretches, suggesting potential SH3 domain binding sites, as have been identified in several guanine nucleotide exchange factors, four consensus sites for tyrosine phosphorylation/SH-2 domain binding, alternative splicing domains, and a leucine zipper motif (reviewed in ref. 18). MAGUKs are currently thought to contribute to the structural organization of components mediating particular signal transduction events (19).

With such a compelling repertoire of signaling domains and the knowledge that loss-of-function mutations of one MAGUK family member (*dlg*) produces an overgrowth phenotype, it seems likely that ZO-1 plays a role in transducing signals from the margin of cell contact to downstream effectors. We present evidence that ZO-1 can accumulate in the cell's nucleus, in addition to sites of cell–cell contact. While the functional significance of the nuclear localization is presently unclear, we demonstrate that these distinct subcellular distributions of ZO-1 are exquisitely sensitive to the state of cell–cell contact.

MATERIALS AND METHODS

Cell Culture and Transfection. All cells (MDCK, MSV-MDCK, LLC-PK1, and CV-1) were maintained in a humidified incubator at 37°C under 10% CO₂ atmosphere in minimal essential medium (DMEM) that was supplemented with 10% fetal calf serum, 50 units of penicillin per ml, 50 µg of streptomycin per ml, and 2 mM L-glutamine. Transfections were carried out as described (20).

Plasmid Construction. The human cDNA for the α+ isoform of ZO-1 (8) was kindly provided by J. Anderson (Yale University) and subcloned into the mammalian expression vector pCB6 (kindly provided by M. Roth, University of Texas Southwestern Medical Center, Dallas; ref. 21). ZO-1 was tagged by incorporating an oligonucleotide encoding 13 C-

Abbreviations: ZO-1, zonula occludens-1; MAGUK, membrane-associated guanylate kinase homologue; NLS, nuclear localization sequence.

[†]To whom reprint requests should be addressed at: Department of Biochemistry and Biophysics, Memorial Sloan-Kettering Cancer Center, New York, NY 10021.

The publication costs of this article were defrayed in part by page charge payment. This article must therefore be hereby marked "advertisement" in accordance with 18 U.S.C. §1734 solely to indicate this fact.

terminal amino acids of the Sendai virus L protein upstream from the stop codon (22).

Indirect Immunofluorescence. Cells were fixed for 25 min with freshly prepared 3.0% paraformaldehyde (wt/vol) in PBS (pH 7.4), supplemented with $\text{Ca}^{2+}/\text{Mg}^{2+}$ and permeabilized with a PBS buffer containing 0.3% Triton X-100 and 0.3% BSA for 5 min. All antibody incubations and washes were carried out using 0.3% BSA in PBS. Cells were incubated for 1 hr at room temperature with either of the following primary antibodies: anti-ZO-1 rat monoclonal (40.76; kindly provided by M. Mooseker, Yale University) or anti-ZO-1 rabbit polyclonal (cat. no. 61-7300, lot no. 40921602; Zymed). For anti-ZO-1 rat monoclonal antibody, the ascites were HPLC-purified; the protein concentration of the IgG fraction was determined to be 0.2 mg/ml. We diluted this antibody 1:30. Anti-ZO-1 rabbit polyclonal antibody (1:300) was affinity-purified by the manufacturer from rabbit antiserum using the 69-kDa fusion protein against which the antibody was raised (23). This fusion protein corresponds to amino acids 463-1109 of the human ZO-1 cDNA (8). Anti-Sendai virus mAb (22) was a kind gift of J. Neubert (Max-Planck-Institut für Biochemie, Martinsried, Germany). Rabbit polyclonal antibody was raised against the 13-aa C terminus of the Sendai virus L protein. Texas Red-conjugated anti-rabbit IgG (Amersham) and fluorescein isothiocyanate-conjugated anti-rat IgG (Southern Biotechnology Associates) secondary antibodies were used for 1 hr at room temperature at a 1:100 dilution. Detergent extraction before fixation experiments were performed as described by Kreis (24). Immunoperoxidase experiments were performed on 10% phosphate-buffered, formalin-fixed, paraffin-embedded tissues according to standard protocols. Signal amplification was performed with a streptavidin/biotin system (Vector Laboratories). Anti-rabbit biotinylated IgG (catalog no. RPN.1004; Amersham) was used at 1:100; streptavidin-horseradish peroxidase (catalog no. ORO3L; Oncogene Science) was diluted 1:200 in PBS. Peroxidase activity was visualized using 3-amino-9-ethylcarbazole (Immunotech). *En face* immunofluorescence images were visualized using the Zeiss Axiophot microscope and photographed using Kodak T-MAX 3200 ASA and Ektachrome films (Eastman Kodak).

SDS/PAGE and Western Blotting. Procedures were carried out using standard methods (25, 26). Blots were incubated with either goat anti-mouse, anti-rabbit, or anti-rat secondary antibodies conjugated to horseradish peroxidase (working dilution 1:2000; Sigma). Labeled proteins were visualized with the enhanced chemiluminescence detection method (ECL; Amersham).

RESULTS

Localization of ZO-1 in Confluent and Nonconfluent Cell Cultures. The tight junction localizing protein ZO-1 characteristically forms a continuous band around the apices of well-differentiated, confluent, polarized epithelial cells in culture [Fig. 1 *A* (MDCK cells) and *C* (LLC-PK1 cells)]. However, under nonconfluent conditions, endogenous ZO-1 can localize to the nucleus in addition to the margin of cell-cell contact (Fig. 1 *B* and *D*). This staining corresponds to the structure labeled with the DNA-binding dye 4',6-diamidino-2-phenylindole (DAPI; data not shown). Moreover, optical sectioning in the *xz* or *xy* direction using a confocal laser scanning microscope confirms that the staining is throughout the nucleus and not just localized to the nuclear membrane (data not shown). This nuclear staining is detected with two different antibodies that recognize distinct portions of the ZO-1 polypeptide; the rat monoclonal antibody R40.76 recognizes the C-terminal region of ZO-1 (Fig. 1) while the rabbit polyclonal antibody 7445 was raised against a bacterial fusion protein encoding the guanylate kinase region (Figs. 2-5). Both antibodies recognize a single 220-kDa molecular species in

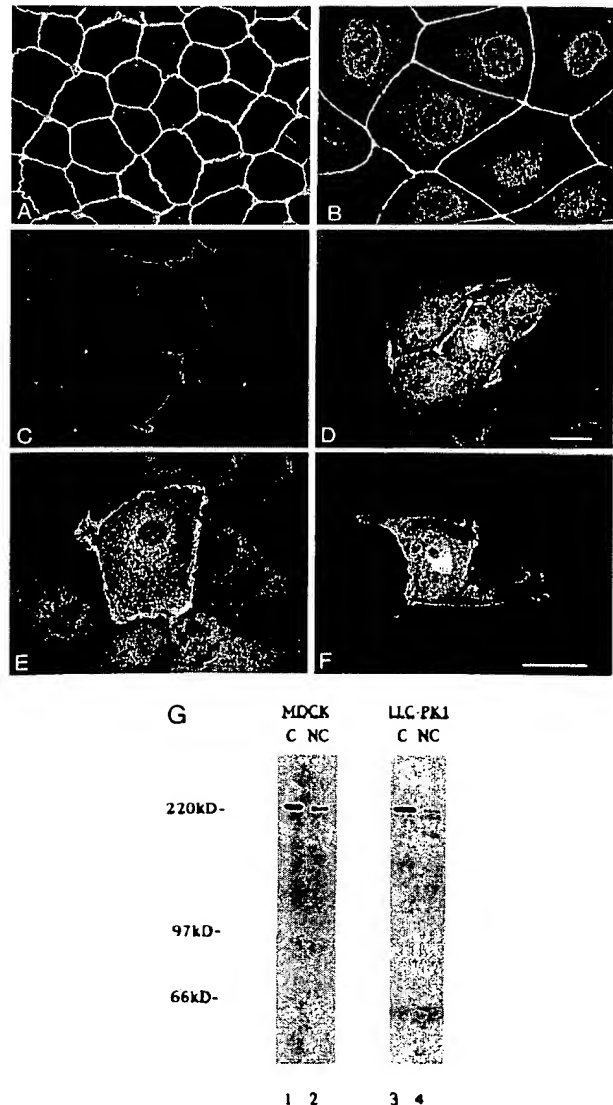


FIG. 1. Subcellular distribution of endogenous and epitope-tagged ZO-1 in confluent and subconfluent polarized epithelial cell cultures. MDCK and LLC-PK1 cells were plated at confluent and subconfluent densities on glass coverslips before being fixed and permeabilized for immunofluorescence analysis using the anti-ZO-1 rat monoclonal antibody R40.76 as described. (*A*) MDCK cells plated and maintained under confluent conditions for at least 4 days; note that ZO-1 localizes exclusively to the apical margin of cell-cell contact. (*B*) MDCK cells plated under subconfluent conditions (cell islands of ~10 cells) and prepared for immunofluorescence analysis between 24 and 48 hr after seeding. Note ZO-1 labeling of nuclei in addition to points of cell-cell contact. (*C* and *D*) LLC-PK1 cells plated at confluent (*C*) and subconfluent (*D*) densities. (*E* and *F*) LLC-PK1 cells transfected with an epitope-tagged human ZO-1 cDNA. (*E*) Transfected cell stained with the anti-Sendai monoclonal antibody. Note that the tagged protein is capable of being localized to the cell margin at points of cell-cell contact. (*F*) Transfected cell detected with an affinity purified anti-Sendai polyclonal antibody. Note that in this transfected cell, epitope tagged ZO-1 localizes to both the nucleus and the margin of cell contact. Bar lengths in *D* and *F* measure 10 and 20 μm , respectively. (*G*) Antibody specificity (antibody 7445) and relative amounts of ZO-1 in confluent (*C*) and nonconfluent (*NC*) cell cultures. Note that there is less ZO-1 per μg of total protein from nonconfluent versus confluent cultures.

MDCK cells by SDS/PAGE and Western analysis (Fig. 1*G*, lanes 1 and 2). ZO-1 migrates as a doublet in LLC-PK1 cells (lanes 3 and 4) and represents the two isoforms (α^+ / α^-)

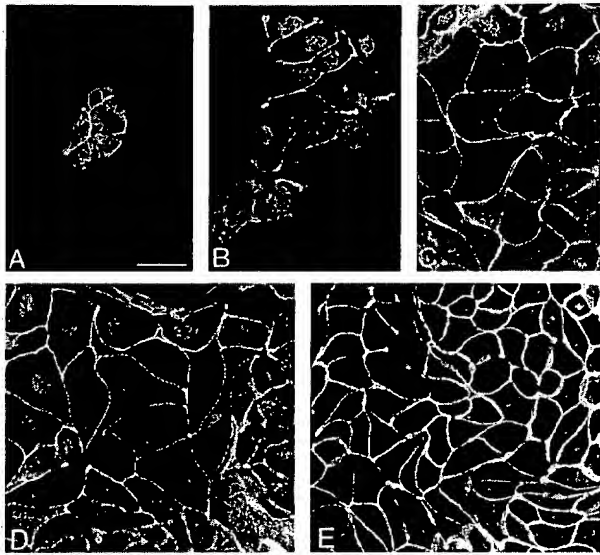


FIG. 2. ZO-1 is accumulated in the nucleus 24 hr after cell plating. MDCK cells were trypsinized and seeded at subconfluent density on glass coverslips. Cells were prepared for immunofluorescence analysis 12 (A), 24 (B), 36 (C), 48 (D), and 72 (E) hr after plating and stained with the anti-ZO-1 polyclonal antibody 7445. Note that nuclear accumulation is detected ≈ 24 hr postplating and persists until cells become increasingly confluent. (Bar = 20 μm .)

known to be expressed in this cell type (23). It is interesting to note that nuclear staining is consistently detected under conditions where cells actually contain less ZO-1 per microgram of total cellular protein (Fig. 1G, compare lanes 1 with 2 and lanes 3 with 4). This would argue against the idea that nuclear localization is a consequence of high levels of endogenous ZO-1 expression.

To provide further evidence that it is ZO-1, and not simply a cross-reactive molecular species, that can localize to the

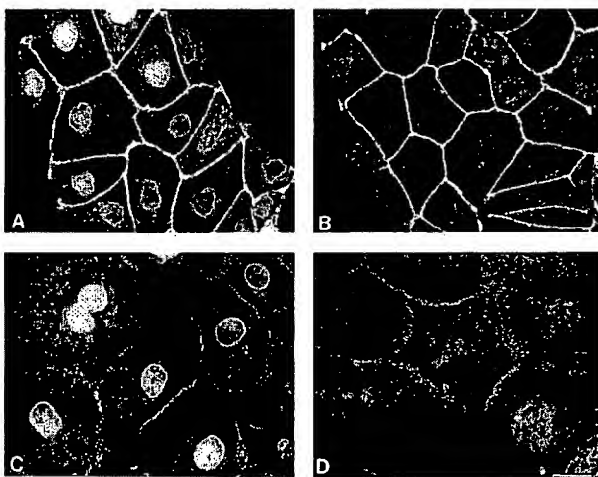


FIG. 3. Nuclear ZO-1 is Triton X-100-extractable. MDCK cells (A and B) and CV-1 cells (C and D) were seeded at nonconfluent densities 48 hr before being prepared for immunofluorescence analysis. The cells in B and D were extracted (0.25% Triton X-100 for 5 min) before being fixed in paraformaldehyde. The cells in A and C were fixed directly in paraformaldehyde. Note that nuclear staining with anti-ZO-1 polyclonal antibody 7445 is clearly visible in fixed cells (A and C), but not in cells that were Triton X-100-extracted before fixation (B and D). Also note that ZO-1 localized to cell-cell contacts appears to be largely Triton X-100-inextractable. Methanol-fixed cells give an immunofluorescence pattern identical to that seen in B and D.

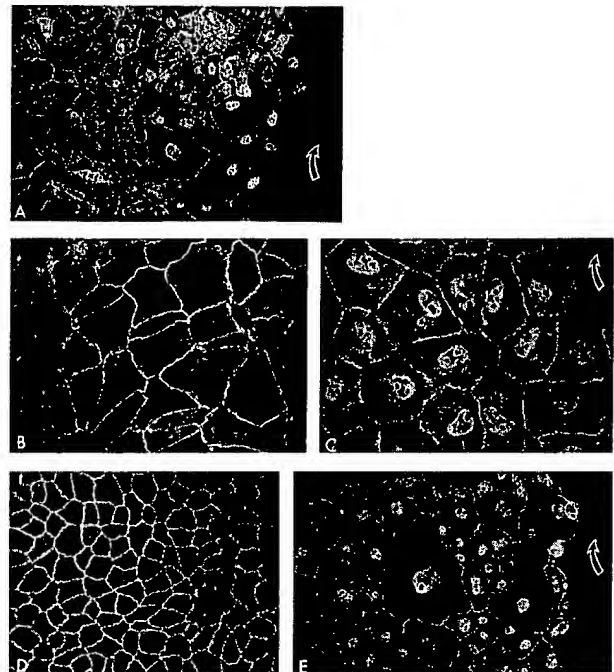


FIG. 4. Conditions that alter the nuclear accumulation of ZO-1. ZO-1 localizations were examined in wounded monolayers of both CV-1 and MDCK cells. CV-1 (A–C) and MDCK (D and E) monolayers were slashed with a 200- μl Pipetman tip to create a discreet 2- to 4-mm "wound." Wounded monolayers were then returned to the incubator for 24 hr before being prepared for immunofluorescence analysis using the anti-ZO-1 polyclonal antibody (7445). (A) Low magnification ($\times 40$) view of wounded CV-1 monolayer. Open arrow shows direction of the wound. Note that only cells proximal to the wound show nuclear labeling. (B and C) The same monolayer as in A, but a different region of the wound, is shown at higher magnification ($\times 63$); B is distal and C is proximal to the wound. (D and E) Wounded MDCK monolayer ($\times 40$); D is distal and E is proximal to the wound site.

nucleus, LLC-PK1 cells were transiently transfected with a cDNA encoding a C-terminal epitope tagged form of ZO-1 ($\alpha+$ isoform). In transfected cells, the tagged protein is incorporated into the margin of cell-cell contact, like the endogenous ZO-1 (Fig. 1E), suggesting that the placement of the epitope tag did not grossly affect ZO-1's ability to localize to its site of ultimate functional residence (data not shown). In some transfected cells, exogenous ZO-1 can be localized to the nucleus in addition to sites of cell-cell contact (Fig. 1F). Interestingly, nuclear labeling observed with the epitope tagged ZO-1 was more often detected in less columnar cells, which often lay in close proximity to an opening in the monolayer. We suggest, therefore, that consistent with endogenous ZO-1 localizations in subconfluent and confluent cells (Fig. 1A–D), epitope-tagged ZO-1 distributions may be dependent on the maturity of the cell monolayer (Fig. 1E and F).

Time Course of ZO-1 Nuclear Accumulation. Clear accumulation of ZO-1 in the nucleus is consistently observed ≈ 24 hr after cell plating (Fig. 2B). While cells that are analyzed at earlier time points appear to contain nuclear ZO-1 (as assessed by confocal analysis; data not shown), this signal is largely obscured by a diffuse cytoplasmic pool (Fig. 2A). Nuclear labeling persists as the cells continue to cover the free spaces on the tissue culture dish (48–56 hr, Fig. 2C and D) and gradually diminishes in intensity as the cells reach confluency (72 hr; Fig. 2E).

Differential Extractability of Nuclear and Junction-Associated ZO-1 Pools. Since ZO-1 is a member of a family of proteins that are thought to participate in the dynamic link between specialized plasma membrane domains and the un-

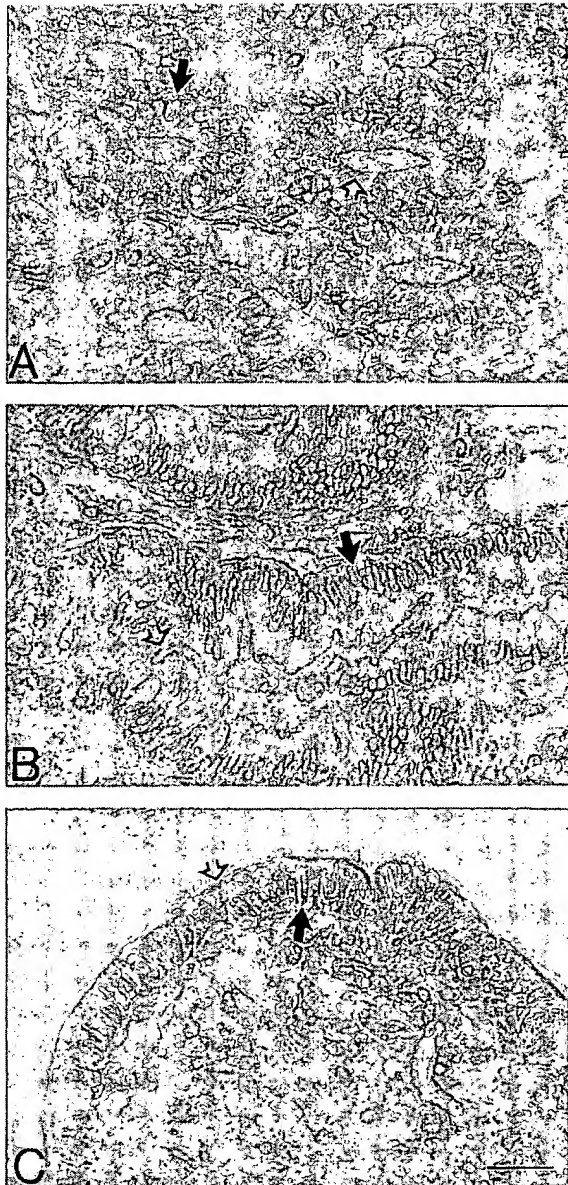


FIG. 5. Nuclear ZO-1 can be detected in intestinal epithelial cells. Paraffin-embedded tissue sections from dog intestine were labeled with anti-ZO-1 polyclonal antibody (7445) using the immunoperoxidase method. ZO-1-specific labeling was examined along the intestinal epithelium lining the crypt-villus axis. (A) Transverse section of intestinal crypts. (B) Longitudinal section along crypt-villus junction. (C) Longitudinal section of the outer region of the villus epithelium. Open arrows point to ZO-1 localizing to junctions; closed arrows point to nuclei. Note that nuclear ZO-1 is only detected at the villus tip. (Bar = 50 μ m.)

derlying cortical cytoskeleton, we wondered whether nuclear ZO-1 is similarly involved in the formation of an extensively cross-linked meshwork of protein-protein interactions. To address this, we chose to explore the relative extractability of both nuclear and junction-associated pools of ZO-1. Nonconfluent MDCK and CV-1 cells were either fixed directly in paraformaldehyde or extracted in a bath of 0.25% Triton X-100 for 5 min before being fixed. We find that the nuclear staining is completely Triton X-100-extractable, while the fraction of ZO-1 present at the junction appears largely inextractable. We suggest, therefore, that the nuclear and junction-associated pools of ZO-1 may participate in structurally and functionally distinct molecular assemblies.

Cell fractionation studies were also undertaken to show that a protein exhibiting the same molecular mobility as ZO-1 could be extracted from a nuclear fraction of subconfluent, but not confluent cells. However, we were unable to estimate the enrichment of ZO-1 in nuclear versus cytoplasmic pools with standard cell fractionation protocols. It is well-known that even the most gentle insult to a cell can cause generalized leaking of nuclear constituents into the cytoplasm and that a number of proteins that clearly localize to the nucleus by immunofluorescence analysis fail to cofractionate with nuclei (for example, see ref. 27). Nuclear fractionation may be especially problematic for studying a protein like ZO-1, whose localization to plasma membrane, cytosolic, and nuclear compartments is highly sensitive to the quality of cell-cell contacts, necessarily modified during any standard fractionation protocol. Moreover, our finding that the nuclear ZO-1 staining is more easily extracted than the junction-associated staining (Fig. 3 and above) further argues against the feasibility of a fractionation study.

Conditions That Affect the Nuclear Accumulation of ZO-1. We wished to find conditions where ZO-1 localization to the nucleus would be stimulated or inhibited. Since subconfluent, but not confluent, cell cultures revealed nuclear ZO-1 staining, we wondered if removing cell-cell contacts by wounding a confluent monolayer could be sufficient to stimulate nuclear accumulation of ZO-1. Fig. 4 shows that in both MDCK cells and CV-1 cells, nuclear localization can be stimulated along the site of wounding (marked with an open arrow). Nuclear staining can often be observed many cell diameters away from the initial wound site and appears to correlate with a zone of cells that must remodel their cell-cell contacts, migrate, and close the wound. Nuclear accumulation was not obvious until ≈ 24 hr after wounding the monolayer, consistent with the time course observed when cells are trypsinized and freshly plated at subconfluent density (Fig. 2B). Moreover, as with the time course in Fig. 2, the nuclear labeling persisted across the zone of wound closure and gradually diminished as cells reached confluent density (56 hr was sufficient time to close a 2-mm wound). We chose to analyze different conditions in which cell-cell contact and proliferative properties would be altered. The ability of several chemical and/or pharmacologic agents to stimulate or inhibit the nuclear localization were tested, but no effects were observed. The phorbol ester, 12-*O*-tetradecanoylphorbol 13-acetate (TPA), phosphatase inhibitor, orthovanadate, EGTA, and serum starvation conditions all failed to enhance nuclear accumulation in subconfluent or confluent monolayers. Hepatocyte growth factor/scatter factor changed the kinetics of this nuclear accumulation, as we could detect nuclear localization after only 12 hr (data not shown). However, hepatocyte growth factor/scatter factor did not appear to increase the amount of ZO-1 accumulated within the nucleus.

Nuclear ZO-1 is Detected Along a Distinct Region of the Intestinal Crypt-Villus Axis. To determine if the nuclear accumulation of ZO-1 occurs *in situ*, we chose to examine a tissue in which cell-cell contacts are formed and lost as a part of a normal cellular life cycle. One such tissue is the intestine, where epithelial cells undergo a well-documented differentiation program. Along the crypt-villus axis, intestinal cells can be divided into regions where cells are proliferating, migrating, differentiating, and undergoing programmed cell death (28). Fig. 5 shows that while ZO-1 tight junction staining can be detected in crypt (Fig. 5A), crypt-villus (Fig. 5B), and outer villus epithelial cells (Fig. 5C; indicated by open arrows), nuclear ZO-1 can only be detected in cells along, approximately, the outer one-fourth of the villus (Fig. 5C; indicated by closed arrows). This represents the region of the villus where cells are preparing to die and exfoliate.

DISCUSSION

Nuclear Localization of ZO-1. In this study, we demonstrate that ZO-1 can be detected in the nucleus under several different experimental conditions. Nuclear labeling was detected by indirect immunofluorescence in three different cell lines (MDCK, LLC-PK1, and CV-1) using two different antibodies against distinct portions of the ZO-1 polypeptide (Figs. 1 and 4). Transient expression of an exogenous, epitope-tagged ZO-1 polypeptide could also be detected in transfected cell nuclei using two distinct epitope tag-specific antibodies. Thus, since this pattern was detected with four different antibodies, we think it unlikely that the nuclear staining represents nonspecific or cross-reactive interactions. Moreover, the nuclear localization appears to correlate with biologically significant events in the maturation of a cell monolayer: nuclear accumulation follows a characteristic time course (Fig. 2), can be stimulated (during the remodeling of cell-cell contacts accompanying wound healing; Fig. 4), and is detected in a tissue whose epithelial cells undergo a loss of cell-cell contact as they execute their normal postmitotic program (Fig. 5).

The nuclear pool of ZO-1 does not appear to be $\alpha+$ / $\alpha-$ isoform specific as the endogenous $\alpha-$ isoform (expressed exclusively in MDCK cells; Fig. 1 *A* and *B*) and the transiently transfected $\alpha+$ isoform can both be localized to the nucleus (Fig. 1 *E* and *F*). It also seems unlikely that the nuclear localization is due to diffusion followed by nonspecific trapping within the nucleus, because ZO-1 is >200 kDa in molecular mass. Proteins of this size would likely require an active transport process through the nuclear pore complex (29). Sequence analysis of ZO-1 reveals two lysine-rich stretches of amino acids, which might serve as putative nuclear localization sequences (NLSs): 95-RRKKK and 490-KKKDVYRR. We have not yet tested whether these sequences are responsible for the nuclear enrichment of ZO-1. Neither of these sequences is identical to simian virus 40 or nucleoplasmin NLSs (29), but the first sequence is very similar to the NLS-containing pentapeptide recently described in a fission yeast DNA polymerase (RKRKK; ref. 30) and a RKRKR NLS recently described for the T-cell protein tyrosine phosphatase p45 (27). It is of interest to note that expression of a cDNA encoding only the first 200 aa of ZO-1 (and including one of these putative NLS, lysine-rich regions) fails to localize to sites of cell contact and accumulates exclusively within the nucleus (A.S.N., A.S.F., and J. Anderson, unpublished data). However, it should be pointed out that ZO-1 need not have an NLS of its own, since many nuclear localizing proteins interact with NLS-containing proteins and gain entry to the nucleus through a "piggyback" mechanism (31, 32). Whether ZO-1 can direct its own nuclear entry or requires an associated partner remains to be determined.

Nuclear Accumulation of ZO-1 is Related to Changes in Cell-Cell Contact. We observed that the nuclear labeling was more robust under nonconfluent rather than confluent conditions. Correlation of this phenomenon with confluency was not peculiar to just one cell type, but rather was generally observed in the three different lines examined: two polarized (MDCK, LLC-PK1) and one nonpolarized cell line (CV-1 cells).

Since the nuclear staining was often more pronounced along the cell-free edge of an island of cells or within a cell lacking neighbors, we hypothesized that the signal for nuclear accumulation might be the loss of or reduction in cell-cell contact, suggesting that the nuclear localization might be inversely related to the extent and/or maturity of cell-cell contacts. This hypothesis is supported by the observation that nuclear accumulation could be stimulated at the sites where a free edge had been generated. The time course for nuclear accumulation after wounding (Fig. 4) was identical to that seen after seeding

cells at subconfluent density (24 hr; Fig. 2), suggesting that the two phenomena are related and that the signaling responsible for nuclear accumulation might be similar.

The localization of ZO-1 to the outer fourth of villus intestinal epithelial cells also supports the hypothesis that nuclear localization is coincident with a change in cell-cell contacts. It is known that cells in this region of the epithelium are preparing for programmed cell death (28) and that tight junctions in particular are undergoing dynamic alterations (33). More specifically, at sites of cellular extrusion, the tight junctions of the nonextruding cells appear to move down the lateral margin of the extruding cell as it extends into the lumen. In this manner, the nonextruding cells "zipper" the epithelium closed thereby preventing transepithelial leaks. It will be of great interest to determine the extent to which nuclear localization of ZO-1 may be related to such changes in tight junction structure accompanying cell death and extrusion events occurring at the villus tip.

Because subconfluent cells are presumably dividing more frequently than confluent cells, it was formally possible that the nuclear labeling could be due to trapping of a cytoplasmic pool of ZO-1 within a reforming nuclear compartment, rather than through a specific nuclear transport mechanism. This seems unlikely for two reasons: (i) ZO-1 is detected in nuclei of the fully differentiated population of enterocytes lining the outer fourth of the intestinal villus, but is not detected in nuclei from the proliferative region located in villus crypts (Fig. 5 *A* and *C*) and (ii) ZO-1 fails to accumulate within the nuclei of a rapidly dividing, virally transformed MSV-MDCK line (data not shown). Furthermore, our failure to correlate nuclear ZO-1 with proliferating cells argues that the nuclear accumulation observed at subconfluency is more a reflection of the state of cell-cell contacts than the proliferative state of the cell.

While it is formally possible that the specific labeling of subconfluent cell nuclei could be due to enhanced antibody accessibility of these nuclei or to preferential masking of ZO-1 epitopes in confluent cell nuclei, we believe that these scenarios are unlikely since the observation has been confirmed with four different antibodies: two ZO-1-specific antibodies that recognize distinct portions of the polypeptide, and two epitope tag-specific antibodies. Furthermore, we have found that an antibody directed against a constitutive nuclear component gives qualitatively similar labeling patterns under both cell density conditions (data not shown).

ZO-1 is a member of a family of MAGUK homologues whose founding member, *dlg*, exhibits tumor suppressor function in the *Drosophila* (9), and therefore has been implicated as a participant in signal transduction from sites of cell-cell contact. It is widely appreciated that the specialized structures at cell contacts (i.e., tight junctions, adherens junctions, and desmosomes) are focal points for cell-cell signaling pathways implicated in growth and differentiation (34, 19). This study demonstrates that ZO-1 can accumulate within a cell's nucleus and that this localization may be inversely related to the extent and/or maturity of cell-cell contact. It is possible that a signal, accompanying a reduction in cell-cell contacts, might be transduced through ZO-1, and that ZO-1 itself might regulate nuclear processes associated with a change in the growth or differentiation status of the cell.

A number of proteins that localize to specialized cell-cell contacts have recently been shown to exhibit transient nuclear localizations. For example, the focal adhesion localizing protein, zyxin, has been localized to nuclei (D. Nix and M. Beckerle, personal communication), and through the action of its LIM domains, has been implicated in protein-protein interactions associated with cellular differentiation (35). The cytoplasmic portion of the Notch receptor has been shown to localize to the nucleus when exogenously expressed (36-38). Notch receptor signaling is believed to regulate the compe-

tence of different cell types to respond to differentiation cues throughout development (39). Moreover, the adherens junction associated protein, β -catenin, has been detected in the nucleus (40). β -catenin (armadillo) is a component of the Wntless/Wnt signaling pathway, which is important for cell fate determination and segment polarity in *Drosophila* and *Xenopus* (41). Recently it has been shown that under very specific conditions, β -catenin and ZO-1 can form an immunoprecipitable complex (42). It will be of great interest to explore the functional consequences of such an association and the extent to which ZO-1 may participate in β -catenin signaling. It is also of interest to note that the dependence of ZO-1 localizations on confluency is not only unique to ZO-1 but has recently been described for the von Hippel-Lindau tumor suppressor gene product (43).

In the above examples of nuclear signaling mediated by plasma membrane-associated proteins, signal transduction mechanisms may not rely upon a cascade of multiple interacting cytosolic components, as has been documented extensively for the growth factor/receptor tyrosine kinase pathways. We propose that signaling events initiated at the cell surface by membrane proteins concentrated in specialized regions of the plasma membrane, such as the junctional complexes, may use a more direct mechanism. In this model, cell surface interactions would promote the dissociation of membrane-associated signaling complexes sequestered at the cytoplasmic faces of the plasma membrane allowing their subsequent translocation into the nucleus.

Note Added in Proof. Recent studies by A. Azim and A. Chishti (St. Elizabeth's Medical Center, Boston; personal communication) provide evidence that another MAGUK family member, hDlg, may localize to cell nuclei in addition to sites along the lateral membrane. The extent to which this nuclear/cell surface localization phenomenon may be a general property of MAGUKs remains to be investigated.

The authors would like to thank James M. Anderson and Tina Van Itallie (Yale University) for advice and for providing the human ZO-1 cDNA; Sylvie Robine and Jean-Jacques Fontaine for help with the paraffin-embedded tissue sections; Jean-Claude Benichou for photographic assistance; and Véronique Collin for general technical assistance. We would especially like to thank Tiziana Crepaldi and Michael Caplan for critically reading the manuscript and all members of the Louvard laboratory for advice, encouragement, and lively discussions. This work was supported by a grant from the J. William Fulbright Foreign Scholars Program, a travel grant from the MS.RJG Fund and a fellowship from the Fondation Curie (C.J.G.), an National Research Service Award DK09261 from the National Institute of Diabetes and Digestive and Kidney Diseases and the Irwin M. Arias Postdoctoral Research Fellowship from the American Liver Foundation (A.S.F.), National Cancer Institute Grant CA66263 (J.M.A.), and by grants from the European community economic BIOMED (BMH4-CT95-0090), the Ligue Nationale Française contre le Cancer, the Human Capital and Mobility (European Community Grant CHRX CT 94-0430), and the Association pour le Recherche sur le Cancer (1825).

- Stevenson, B. R., Siliciano, J. D., Mooseker, M. S. & Goodenough, D. A. (1986) *J. Cell Biol.* **103**, 755–766.
- Balda, M. S. & Anderson, J. M. (1993) *Am. J. Physiol.* **264**, C918–C924.
- Howarth, A. G., Hughes, M. R. & Stevenson, B. R. (1992) *Am. J. Physiol.* **262**, C461–C469.
- Itoh, M., Nagafuchi, A., Yonemura, S., Kitani-Yasuda, T., Tsukita, S. & Tsukita, S. (1993) *J. Cell Biol.* **121**, 491–502.
- Gumbiner, B. M., Stevenson, B. & Grimaldi, A. (1988) *J. Cell Biol.* **107**, 1575–1587.
- Siliciano, J. D. & Goodenough, D. A. (1988) *J. Cell Biol.* **107**, 2389–2399.
- Balda, M. S., Gonzalez-Mariscal, L., Contreras, R. G., Macias-Silva, M., Torres-Marquez, M. E., Garcia-Sainz, J. A. & Cereijido, M. (1991) *J. Membr. Biol.* **122**, 193–202.
- Willott, E., Balda, M. S., Fanning, A. S., Jameson, B., Van Itallie, C. & Anderson, J. M. (1993) *Proc. Natl. Acad. Sci. USA* **90**, 7834–7838.
- Woods, D. F. & Bryant, P. J. (1991) *Cell* **66**, 451–464.
- Jesaitis, L. A. & Goodenough, D. A. (1994) *J. Cell Biol.* **124**, 949–961.
- Cho, K.-O., Hunt, C. & Kennedy, M. B. (1992) *Neuron* **9**, 929–942.
- Kistner, U., Wenzel, B. M., Veh, R. W., Cases-Langhoff, C., Garner, A. M., Appeltaure, U., Voss, B., Gundelfinger, E. D. & Garner, C. C. (1993) *J. Biol. Chem.* **268**, 4580–4583.
- Ruff, P., Speicher, D. W. & Husain-Chisti, A. (1991) *Proc. Natl. Acad. Sci. USA* **88**, 6595–6599.
- Kim, S. (1995) *Curr. Opin. Cell Biol.* **7**, 641–649.
- Lue, R., Marfatia, S. M., Branton, D. & Chisti, A. H. (1994) *Proc. Natl. Acad. Sci. USA* **91**, 9818–9822.
- Kim, E., Niethammer, M., Rothschild, A., Jan, Y. N. & Sheng, M. (1995) *Nature (London)* **378**, 85–88.
- Kornau, H.-C., Schenker, L. T., Kennedy, M. B. & Seeburg, P. H. (1995) *Science* **269**, 1737–1740.
- Anderson, J. M., Balda, M. S. & Fanning, A. S. (1993) *Curr. Opin. Cell Biol.* **5**, 772–778.
- Fanning, A. S., Lapierre, L. A., Brecher, A. R., Van Itallie, C. M. & Anderson, J. M. (1996) *Curr. Top. Membr.* **43**, 211–235.
- Arpin, M., Friederich, E., Algrain, M., Vernel, F. & Louvard, D. (1995) *J. Cell Biol.* **127**, 1995–2008.
- Brewer, C. & Roth, M. G. (1991) *J. Cell Biol.* **114**, 413–421.
- Einberger, H., Mertz, R., Hofschneider, P. H. & Neubert, J. (1990) *J. Virol.* **64**, 4274–4280.
- Willott, E., Balda, M. S., Heintzelman, M., Jameson, B. & Anderson, J. M. (1992) *Am. J. Pathol.* **138**, C1119–C1124.
- Kreis, T. E. (1987) *EMBO J.* **6**, 2597–2606.
- Laemmli, U. K. (1970) *Nature (London)* **227**, 680–685.
- Towbin, H., Staehelin, T. & Gordon, J. (1979) *Proc. Natl. Acad. Sci. USA* **76**, 4350–4354.
- Lorenzen, J. A., Dadabay, C. Y. & Fischer, E. H. (1995) *J. Cell Biol.* **131**, 631–644.
- Gordon, J. I. & Hermiston, M. L. (1994) *Curr. Opin. Cell Biol.* **6**, 795–803.
- Forbes, D. J. (1992) *Annu. Rev. Cell Biol.* **8**, 495–527.
- Bouvier, D. & Baldacci, G. (1995) *Mol. Biol. Cell* **6**, 1697–1705.
- Dingwall, C., Sharnick, S. V. & Laskey, R. A. (1982) *Cell* **30**, 449–458.
- Zhao, L.-T. & Padmanabhan, R. (1988) *Cell* **55**, 1005–1015.
- Madara, J. L. (1990) *J. Membr. Biol.* **116**, 177–184.
- Tsukita, S., Itoh, M. A. N., Yonemura, S. & Tsukita, S. (1993) *J. Cell Biol.* **123**, 1049–1053.
- Schmeichel, K. L. & Beckerle, M. C. (1994) *Cell* **79**, 211–219.
- Lieber, T., Kidd, S., Alcamo, E., Corbin, V. & Young, M. W. (1993) *Genes Dev.* **7**, 1949–1965.
- Fortini, M. E., Rebay, L., Caron, L. A. & Artavanis-Tsakonas, S. (1993) *Nature (London)* **365**, 555–557.
- Struhl, G., Fitzgerald, K. & Greenwald, I. (1993) *Cell* **74**, 331–345.
- Artavanis-Tsakonas, S., Matsuno, K. & Fortini, M. E. (1995) *Science* **268**, 225–232.
- Funayama, N., Fagotto, F., McCrea, P. & Gumbiner, B. M. (1995) *J. Cell Biol.* **128**, 959–968.
- Siegfried, E. & Perrimon, N. (1994) *BioEssays* **16**, 395–403.
- Rajasekaran, A. K., Hojo, M., Huima, T. & Rodriguez-Boulant, E. (1996) *J. Cell Biol.* **132**, 451–463.
- Lee, S., Chen, D. Y. T., Humphrey, J. S., Gnarr, J. R., Linehan, W. M. & Klausner, R. D. (1996) *Proc. Natl. Acad. Sci. USA* **93**, 1770–1775.

Sugar Tests Detect Celiac Disease Among First-Degree Relatives

Edgardo Smecuol, M.D., Horacio Vazquez, M.D., Emilia Sugai, Ph.D., Sonia Niveloni, M.D., Silvia Pedreira, M.D., Ana Cabanne, M.D., Alcira Fiorini, M.D., Zulema Kogan, M.D., Eduardo Mauriño, M.D., Jon Meddings, M.D., and Julio C. Bai, M.D.

Small Intestinal Section, Clinical Service, Pathology Service, and Endoscopy Service, Hospital de Gastroenterología, Buenos Aires, Argentina; and GI Research Group, University of Calgary, Calgary, Alberta, Canada

OBJECTIVES: First-degree relatives of patients with celiac disease are at high risk for developing the disease themselves. Detection of serum antibodies and intestinal permeability tests have been useful to identify candidates for intestinal biopsies. Recently it was demonstrated that abnormal sucrose permeability is a very sensitive marker of active disease. Our objectives in this prospective study were (1) to assess the screening value of permeability tests, and (2) to compare the usefulness of these markers with that of the celiac disease-related serology in screening for celiac disease in a cohort of first-degree relatives of well-known patients.

METHODS: We performed sugar tests in 66 first-degree relatives of probands. Subjects ingested 450 ml of a solution containing sucrose (100 g), lactulose (5 g), and mannitol (2 g). Subsequently, a complete overnight urine collection was obtained. Measurement of sugars was performed by high-performance liquid chromatography. All relatives were evaluated for antigliadin (type IgA and IgG) and endomysial antibodies and subjects positive for any test underwent intestinal biopsy.

RESULTS: Twelve relatives were diagnosed as having small intestinal mucosal atrophy. Increased sucrose permeability was detected in 9 (75%) of these patients. Four false-positive determinations were found but all had gastric erosions, which is known to increase sucrose permeability independently of duodenal damage. Increased lactulose/mannitol ratios were observed in all new celiac patients. An additional nine relatives had positive results; however, four of them did not accept intestinal biopsy and the remaining five did not seem to have histological evidence of disease. Endomysial antibodies were detected in 11 of 12 patients and no false-positive cases were observed. Antigliadin antibodies were 75% sensitive and 88% specific.

CONCLUSIONS: Our study demonstrated that screening using the endomysial antibody test is highly sensitive and specific for detecting celiac disease; however, almost 10% can be missed. The addition of lactulose/mannitol perme-

ability testing to the screening protocol allowed us to detect all relatives who actually presented with evidence of gluten sensitivity. Sucrose permeability exhibited a lower sensitivity; however, it did detect other endoscopically visible lesions. (*Am J Gastroenterol* 1999;94:3547-3552. © 1999 by Am. Coll. of Gastroenterology)

INTRODUCTION

Screening for new celiac patients is mandatory because early diagnosis and treatment may prevent the long-term complications of the disease such as cancer and lymphoma (1, 2), avoid complications of severe osteoporosis (3), and restore occult nutritional deficiencies (4). First-degree relatives of patients with celiac disease (CD) are at high risk for developing CD themselves (5-9). Family studies have demonstrated that 10% to 15% of these relatives have intestinal mucosal atrophy (5). There is general agreement that approximately 50% of these new patients have no symptoms at the time of diagnosis (6, 7). Recent studies have shown that a significant proportion of the remaining relatives have features consistent with latent or potential gluten sensitivity (8, 9).

Screening protocols have included a variety of tools to identify candidates that might benefit from intestinal biopsy. A general consensus considers that antigliadin (AGA) and endomysial (EmA) antibodies are the most useful screening tools (10-12). However, CD-related serology identifies subjects with minimal features of gluten sensitivity (10). Furthermore, these markers do not identify all subjects with gluten intolerance. For instance, CD occurs in patients without increased specific antibodies and in subjects with selective/total antibody deficiency syndromes (13, 14).

Abnormal intestinal permeability has been found in a very high proportion of patients with active CD. Permeability was also evaluated in the screening of first-degree relatives (15-21). Uil *et al.* (22) and Vogelsang *et al.* (23) have suggested that the lactulose/mannitol (lac/man) ratio is useful for family screening. Nevertheless, the screening value of these tests has not been confirmed by other investigators

who have found normal intestinal permeability in a high number of new patients screened from the general population (24). Recently, we have demonstrated that sucrose, a disaccharide with a molecular size and permeation pathway similar to lactulose and which is rapidly destroyed in the intestine by sucrase-isomaltase, was 93% sensitive for active CD (25). It remains to be demonstrated whether increased sucrose permeability can detect patients with minimal histological evidence of the disease and whether it is useful for screening in high-risk groups. Furthermore, information about the comparative screening value of permeability probes and CD-related serology is not available.

Our aim in this prospective study was to assess the screening value of sugar permeability tests (consisting of a cocktail of sucrose, mannitol, and lactulose) in a cohort of first-degree relatives of well-known celiac patients. We additionally compared their performance with that of more traditional immunological markers.

MATERIALS AND METHODS

Patients

We evaluated 66 first-degree relatives (37 females; mean age 32 yr; range 7–74 yr) of 45 well-established CD patients who attended the Small Bowel Section of the Hospital de Gastroenterología in Buenos Aires between December 1996 and October 1997. Of the 66 relatives, 16 were children, 38 parents, and 12 siblings of the probands. CD was diagnosed according to currently accepted criteria based on the presence of mucosal atrophy on small bowel biopsy in the context of being a first-degree relative of the proband. All subjects were informed of the purpose of the study and agreed to participate accepting the eventual possibility of endoscopy and intestinal biopsy. The study was approved by the Research and Ethical Committees of the Gastroenterology Hospital.

Study Design

All relatives underwent a clinical evaluation, nutritional assessment, and routine blood tests. All subjects performed sugar permeability tests after ruling out the intake of non-steroidal anti-inflammatory agents, acetylsalicylic acid, or alcoholic beverages in the 2 weeks before the study. At the same time all relatives were evaluated for CD-related serology (IgA and IgG AGA and EmA antibodies). Patients with positive IgG AGA and negative for IgA AGA and EmA were quantitatively evaluated for total and IgA serum gamma globulin. Finally, subjects positive for any test were submitted to an upper GI endoscopy with distal duodenal biopsies.

Sugar Tests

A test solution containing 5 g of lactulose (Technilab, Montreal, Quebec, Canada), 2 g of mannitol (Sigma, St. Louis, MO), and 100 g of sucrose in 450 ml of water (osmolality approximately 1800 mOsm/L) was ingested by relatives at

bedtime after a 4-h fast. Subjects voided before drinking the solution and then collected all urine, including the first morning void, in a preweighted container with 5 ml of 10% thymol in isopropanol. The urine was vigorously mixed, total volume recorded, and aliquots rapidly frozen for a deferred analysis.

Analytical Methods

PERMEABILITY ASSAYS. Ten-milliliter samples of urine were decanted for analysis. Cellobiose was added as an internal standard. The samples were deionized by adding 1 g of a 1:1.5 (wt:wt) mixture of Amberlite IR-120 and IRA-400 resin (BDH chemicals, Toronto, ON, Canada). The supernatant was then filtered through a 45- μ m millipore filter (Millipore, Bedford, MA). Samples were separated on a Dionex Carbopac MA-1 anion exchange column (Dionex, Ontario, Canada) in a Dionex high-performance liquid chromatography using 520 mmol/L NaOH as the isocratic mobile phase. Peak identification was performed using pulsed amperometric electrochemical detection on a gold electrode. Quantitation was performed using known standards at multiple concentrations, with linear interpolations between concentrations. As electrochemical detection of carbohydrates is sensitive, samples were diluted after the addition of the internal standard. If these dilutions were not satisfactory for proper analysis, adjustments to the dilutions were performed so that the sucrose, mannitol, and lactulose concentrations decreased within the range of the standards. The fractional excretion of lactulose and mannitol was calculated from the urinary concentrations of these sugars; the lac/man ratio is reported. The total mass of sucrose excreted in the overnight urine sample is reported as calculated from its urinary concentration and the total volume of urine produced.

CD-RELATED SEROLOGY. Antigliadin antibodies, type IgA and IgG, were measured by the micro-ELISA method, as previously described (10). The upper limits of normal were 14 arbitrary units/ml and 20 arbitrary units/ml for AGA IgA and IgG, respectively. Endomysial antibody was determined using the indirect immunofluorescence method as previously described (10).

INTESTINAL BIOPSIES. All biopsies were performed following a standard protocol through a videoendoscope (Fujinon EG-300 HR; Fujinon, Japan). At least three samples from the distal duodenum and two from the stomach (antrum and body) were obtained using conventional endoscopic forceps (open cup: 8 mm). Samples were carefully orientated on filter paper (Millipore) and fixed in 10% formalin. Biopsies were embedded in paraffin wax, cut in sections 5 μ m thick, and stained with hematoxylin and eosin. Small bowel biopsies were evaluated by observers unaware of the clinical and endoscopic findings.

SMALL BOWEL HISTOLOGY. Histological characteristics of the duodenal mucosa were classified, according to previous studies (10, 25), into four types depending on the

Table 1. Clinical Features of First-Degree Relatives of CD Patients and 12 Newly Diagnosed CD Patients (X SD)

Characteristics	First-Degree Relatives		New CD Patients		<i>p</i> Value
No. (female/male)	54 (29/25)		12 (8/4)		
Mean age (range, yr)	32 (7–63)		33 (10–74)		
Body mass index	23.7	4.3	20.9	3.1	0.052
Body weight (kg)	70.2	41.2	50.2	9.6	0.03
Laboratory tests					
Hemoglobin (g/dl)	13.3	3.0	11.3	4.1	0.051
Albumin (g/ml)	3.9	0.5	3.4	0.6	
Calcium (g/dl)	8.1	1.1	7.6	0.7	
Serum antibodies					
(number of patients with abnormal results)					
AGA IgA	0/54		5/12		
AGA IgG	5/54		9/12		
EmA	0/54		11/12		
Sucrose excretion					
median (mg)	104.2		278.8		0.00001
95% CI	82.2–126.3		33.6–423.9		
Lac:man ratio					
median	0.019		0.101		0.00003
95% CI	0.016–0.021		0.065–0.143		

following features: structure of villi, crypt:villus ratio, infiltration of the lamina propria, and epithelial cell features. Type I was defined as normal mucosa; type II shortened and widened villi with a decrease in crypt:villus ratio as compared to type I and increased cellularity of the lamina propria. Type III was defined as very short or almost absent villi, with a reversed crypt:villus ratio, cuboidal or pseudostratified epithelium, tortuous and long crypts, and a dense mononuclear infiltration of the lamina propria. Type IV represented complete villous atrophy.

Statistical Analysis

Results are presented as mean SEM or median and 95% confidence interval. Statistical comparison of the permeability tests was performed using the Mann-Whitney U test.

Sensitivity, specificity, and predictive values were determined according to conventional formulas.

RESULTS

Clinical Assessment

According to our protocol, 12 relatives (18%) were determined to have intestinal mucosal atrophy. Tables 1 and 2 illustrate the clinical features of this population and compare them with those of the nonceliac relatives. CD was diagnosed two times more frequently in female than in male relatives. It can be observed that one-third of new celiacs were completely asymptomatic and that another one-third presented major symptoms related to severe malabsorption. Body weight and body mass index were significantly reduced in the new celiac patients compared with nonatrophic controls. Serum albumin was borderline lower in patients than in controls ($p = 0.051$). No differences were observed in the concentration of Hb and total serum calcium between new patients and those relatives without atrophy.

Histological Evaluation

Biopsy procedures were performed in 28 relatives who had an abnormal screening test (15 had abnormal serology; 23 relatives had an abnormal lac/man ratio and 14 increased had sucrose excretion). Fourteen relatives had a combination of more than one parameter abnormal. Four relatives refused intestinal biopsy. None of them were EmA positive and one had severe serum IgA deficiency. Twelve relatives had small intestinal mucosal atrophy (one type II, two type III, and nine type IV). The patient with intestinal mucosa type II had an intraepithelial lymphocyte count of 32%. The remaining 16 relatives who underwent biopsy presented a normal mucosa (type I).

CD-Related Serology

IgA and IgG AGAs detected five and nine patients, respectively. IgA AGA had no false-positive results, but IgG was

Table 2. Descriptive Analysis of the 12 Patients Newly Diagnosed of Celiac Disease

Patient	Age	Clinical Status	BMI	Permeability Tests		Serological Studies			Biopsy Type
				Lac/man	Sucrose (mg)	AGA-IgA (Au)	AGA-IgG (Au)	EmA	
1	25	Subclinical	20.7	0.135	366.9	58	26		IV
2	11	Classical	21.5	0.062	88.6	6	25		IV
3	42	Asymptomatic	17.9	0.027	187.4	9	58		IV
4	10	Asymptomatic	17.7	0.04	249.2	7	46		IV
5	35	Classical	20.3	0.261	860.3	2	5		IV
6	22	Classical	18.2	0.095	248.1	20	58		IV
7	45	Subclinical	20.2	0.113	467.5	15	41		III
8	31	Subclinical	24.2	0.136	0.6	13	47		III
9	35	Subclinical	19.4	0.058	187.9	6	10		IV
10	13	Asymptomatic	23.8	0.059	41.0	6	14		II
11	42	Classical	22.1	0.083	361.7	18	20		IV
12	74	Asymptomatic	24.1	0.143	336.2	32	28		IV

Clinical status was classified as classical malabsorption, subclinical disease (chronic anemia, gynecological, or obstetrical disorders, oral ulcers, etc.) or asymptomatic. Biopsies were evaluated as described in the Methods section. BMI = body mass index. Normal sucrose excretion: 180 mg. Normal lac/man ratio = 0.025. AGA-IgA and AGA-IgG antigliadin antibodies type IgA and IgG in arbitrary units (AU) (normal values: 15 and 20 AU/ml, respectively). Type of biopsy according to a previous studies (see Methods section). Data in bold letters mean positive results.

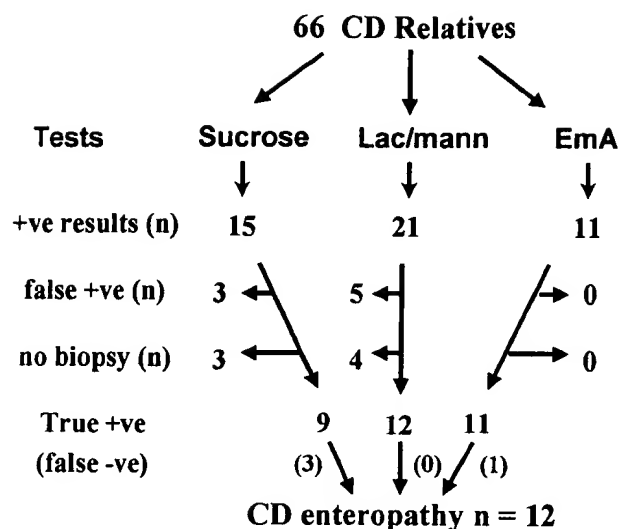


Figure 1. Results of permeability tests (sucrose and lactulose/mannitol [lac/man]) and endomysial antibody (EmA) performed in the cohort of relatives studied and referred as number (n) of subjects with positive (+ve) or negative (-ve) results. Note: The six cases who were sucrose negative presented normal lac/man tests.

positive in six of the nonceliac relatives. Endomysial antibody exhibited the best performance in screening for new CD patients. Thus, overall 11 of 12 patients (92%) were positive for this test and no false positives were found. The only patient who was EmA negative had a total IgA serum level within the normal range.

Sucrose Permeability

Median sucrose permeability in non-CD relatives was significantly lower than that of newly diagnosed CD patients ($p = 0.00001$) (Figs. 1, 2, and Table 1). In Figure 2 the vertical axis represents the total mass of sucrose excreted after ingestion of the test solution. The dotted line represents the upper limit of normal as it was previously defined (25).

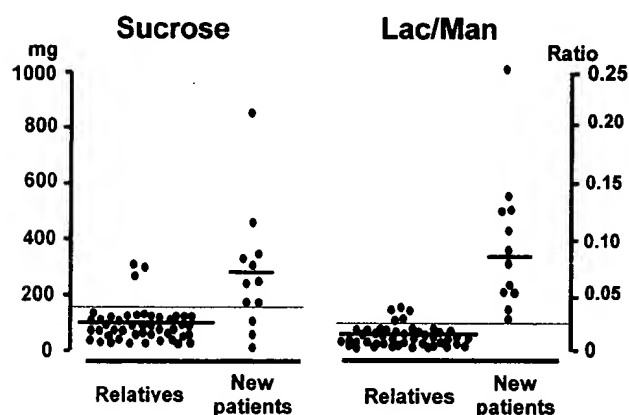


Figure 2. Sucrose excretion rates and lac/man ratio in non-CD relatives and in newly diagnosed CD patients. Dotted line indicates the upper normal limit. Thick horizontal bar represents the mean value of the populations.

Table 3. Individual Statistical Value of Immunological and Permeability Tests in Screening First-Degree Relatives of Celiac Disease Patients

	AGA-IgA (%)	AGA-IgG (%)	EmA (%)	Sucrose Test (%)	Lac/man Ratio (%)
Sensitivity	41	75	92	75	100
Specificity	100	88	100	91	83
Positive predictive value	100	60	100	69	60
Negative predictive value	88	94	98	94	100

Nine of 12 relatives (75%) with CD clearly had abnormal sucrose excretion on presentation. The remaining three patients had normal rates of sucrose excretion, but it is important to note that one of these three was the patient with only minimal alterations in duodenal morphology (type II). False-positive results, in terms of villous atrophy, were detected in three subjects. However, all of these patients had significant gastric damage found at endoscopy (gastric erosions). Finally, three relatives with sucrose excretion above the normal range did not agree to undergo small bowel biopsy.

Lactulose/Mannitol Test

Small intestinal permeability was increased in all new CD patients (12 of 12). These data are shown in Figure 2 and the mean data are also presented in Table 1. As illustrated, CD patients had a significantly increased mean lac/man ratio compared to non-CD relatives ($p = 0.00003$). However, histological findings did not confirm CD in five relatives with high lac/man ratios (false-positive cases). Although these relatives had abnormal permeability, the magnitude of this was less than that observed in patients with CD. Interestingly, the patient with minimal histological changes was detected by both the lac/man ratio and EmA, but not by abnormal sucrose permeability or AGA tests. Finally, four subjects with increased lac/man ratios did not accept duodenal biopsy.

Comparative Diagnostic Value of Immunological and Sugar Tests

The sensitivity, specificity, and positive and negative predictive values of the sucrose test, lac/man ratio, AGA and EmA antibodies, as well as the individual tests in the screening for new patients are reported in Tables 3 and 4. The lac/man test exhibited the highest sensitivity and negative predictive value. Both AGA IgA and EmA had absolute specificity and positive predictive values. Table 4 shows data on the statistical value of combinations of two tests. All CD patients were detected by the combination of EmA and lac/man ratios. However, using both tests prompted an unnecessary biopsy in nine nonatrophic relatives.

Table 4. Statistical Value of the Combination of Two Tests

	AGA-IgA AGA-IgG (%)	EmA AGA-IgA AGA-IgG (%)	Sucrose Test L/M Ratio (%)	EmA Sucrose Test (%)	EmA L/M Ratio (%)
Sensitivity	75	92	100	92	100
Specificity	88	88	75	91	83
Positive predictive value	60	64	48	69	65
Negative predictive value	94	98	100	98	98

DISCUSSION

Screening for CD in high-risk groups is mandatory to prevent late complications of the disease. First-degree relatives are the paradigm of a high risk who present with a wide spectrum of symptoms; 50% can be completely asymptomatic. Because intestinal biopsy for all members of this population is impractical, a clinically useful screening protocol is necessary. Serological tests have proved to be the most cost effective and available tools for this purpose). However, several important issues still remain unsolved.

When the reported variability in detection rates for EmA and the well-recognized false-negative results for serum antibody testing are taken into consideration, there is a significant possibility of a number of patients with CD that will remain undiagnosed with current screening (13, 14). Permeability testing, such as lac/man ratios (18, 21–23, 25) or sucrose (25), have been shown to be highly sensitive for active CD. However, information on their performance (either alone or in combination with serological tests) in the screening of high-risk populations has been missing. The present cross-sectional study attempted to explore the true magnitude of the gluten sensitivity iceberg in first-degree relatives of CD patients. On the basis of a screening protocol using immunological and sugar permeability tests, we identified CD in 18% of first-degree relatives of patients. Two-thirds were either asymptomatic or had a subclinical course before diagnosis. Endomysial antibody testing was highly sensitive and absolutely specific for a new patient. Conversely, AGAs were much poorer than the other tests. The lac/man ratio, which has not been previously tested in a large cohort, showed 100% sensitivity but false-positive cases were detected. Sucrose permeability exhibited moderate sensitivity (75%) and high specificity (91%). Finally, the combination of EmA and lac/man ratios allowed the identification of all new celiacs; however, the combination precipitated intestinal biopsy in 7.5% of the population that subsequently appeared not to have CD.

The determination of the prevalence of CD in first-degree relatives has been addressed by several groups, including ourselves (5–10). Only intestinal biopsy of the complete cohort allows the identification of all new patients. However, this kind of screening is clinically impractical. Therefore, most screening studies are based on the very high positive predictive value of CD-related serology. In this case the true prevalence of CD can be underestimated by false-

negative cases where no clinical or serological markers indicate the necessity of biopsy. Taking into consideration the published sensitivity and specificity of EmA, the best serological test, we can estimate a false-negative rate of 10%. Previous studies have also suggested that abnormal permeability, as determined by a lac/man ratio can achieve a sensitivity of 100% (21, 22). Taking advantage of this finding, and that permeability tests are not affected by the same factors that limit serological testing, we used permeability tests to screen the relative population. In fact our data suggest that the actual false-negative rate for serological is approximately 10%.

In the present study, sucrose permeability was less sensitive than previously reported in the diagnosis of CD (25). We believe that this discrepancy is related to the severity or extent of the mucosal lesion. It was clear from our data that patients with normal sucrose permeability also had less severe clinical profiles (two had an asymptomatic clinical course and the other presented with a subclinical form). Permeability testing also identified a number of false-positive cases, at least when positive was defined as histological evidence of CD. It is well reported that sucrose permeability is increased in the presence of erosive gastric disease and this was apparent in our population as well (26, 27). In a similar manner, small intestinal permeability can be abnormal in a wide variety of conditions including acute enteritis, nonsteroid antiinflammatory intake, alcohol consumption, and inflammatory bowel disease (28, 29). Previous studies have detected a cohort of nonatrophic relatives who exhibit increased lac/man ratios but lower ratios than those of CD. van Elburg *et al.* (30) and Vogelsang *et al.* (23) observed abnormal intestinal permeability in 30% and 70% of healthy family members, respectively. Our study demonstrated that 9% of the relatives who seem not to have CD also have an abnormal lac/man ratio confirming these observations. The significance of this finding in relatives with normal villous architecture is unclear. It has been suggested that this subtle permeability defect could be an initiating event in the pathogenic process of gluten sensitivity (30–32). Increased intestinal permeability may facilitate the interaction of gluten with the intestinal immune system triggering the local immunopathological events characteristics of gluten sensitivity. Only a longitudinal study of those nonatrophic relatives who exhibit abnormal intestinal permeability will be able to determine whether these individuals will eventually develop

CD. Interestingly, we have recently detected that relatives who presented a normal intestinal mucosa but serological evidence of gluten sensitivity at an initial assessment can later develop a severe enteropathy (Niveloni *et al.*, unpublished observations).

In conclusion, our cross-sectional study has allowed us to obtain an estimation of the size of the celiac population among first-degree relatives. Two-third of patients presented with either an asymptomatic or a subclinical course. We confirm previous studies highlighting the role of EmA in the screening of new patients. In addition, the lac/man ratio was very helpful to characterize the population and detect patients missed by serology. The sucrose permeability test was less effective, probably because patients presented with less extensive mucosal disease, and it was predictably less specific as other common conditions can increase gastric permeability. An interesting population was also identified. This consisted of patients with clearly abnormal small intestinal permeability, but no evidence of CD on biopsy. Whether these patients represent a very early form of CD, an abnormality that precedes CD, some other small intestinal disease or true false-negative results cannot be answered by this study and will require additional investigations and follow-up.

Reprint requests and correspondence: Julio C. Bai, M.D., Hospital de Gastroenterología, "Dr. Carlos Bonorino Udaondo," Caseros 2061, 1264 Buenos Aires, Argentina.

Received Feb. 12, 1999; accepted July 6, 1999.

REFERENCES

- Holmes GKT, Prior P, Lane MR, et al. Malignancy in coeliac disease—effect of a gluten free diet. *Gut* 1989;30:333–8.
- Marsh M. Is celiac disease (gluten sensitivity) a premalignant disorder? *J Pediatr Gastroenterol Nutr* 1997;24:S25–7.
- Bai JC, Gonzalez D, Mautalen C, et al. Long-term effect of gluten restriction on bone mineral density of patients with coeliac disease. *J Clin Gastroenterol* 1997;25:421–5.
- Smecuol E, Gonzalez D, Mautalen C, et al. Longitudinal study on the effect of treatment on body composition and anthropometry of celiac disease patients. *Am J Gastroenterol* 1997;92:639–42.
- Maki M, Pekka C. Coeliac disease. *Lancet* 1997;349:1755–9.
- Auricchio S., Mazzacca G, Tosi R, et al. Coeliac disease as a familial condition: Identification of asymptomatic coeliac patients within family groups. *Gastroenterol Intern* 1988;1:25–31.
- Corazza GR, Velentini RA, Frisoni M. Gliadin immune reactivity is associated with overt and latent enteropathy in relatives of celiac patients. *Gastroenterology* 1992;103:1517–22.
- Vazquez H, Cabanne A, Sugai E, et al. Serological markers identify histologically latent coeliac disease among first-degree relatives. *Eur J Gastroenterol & Hepatol* 1996;8:15–21.
- Dezi R, Niveloni S, Sugai E, et al. Gluten sensitivity in the rectal mucosa of first-degree relatives of celiac disease patients. *Am J Gastroenterol* 1997;92:1326–30.
- Vazquez H, Sugai E, Pedreira S, et al. Screening for asymptomatic celiac sprue in families. *J Clin Gastroenterol* 1995;21:130–3.
- Catassi C, Ratsch IM, Fabiani E, et al. High prevalence of undiagnosed coeliac disease in 5280 Italian students screened by anti gliadin antibodies. *Acta Paediatr* 1995;84:672–6.
- Valdimarsson T, Franzer L, Grodzinsky E, et al. Is small bowel biopsy necessary in adults with suspected celiac disease and IgA anti-endomysium antibodies? *Dig Dis Sci* 1996;41:83–7.
- Cataldo F, Marino V, Ventura A, et al. Prevalence and clinical features of selective immunoglobulin A deficiency in coeliac disease: An Italian multicentre study. Italian Society of Paediatric Gastroenterology and Hepatology (SIGEP) and "Club del Tenue" Working Groups on Coeliac Disease. *Pediatr Gastroenterol Nutr* 1996;23:504–6.
- Heneghan MA, Stevens FM, Cryan EM, et al. Celiac sprue and immunodeficiency states: A 25-year review. *Gut* 1998;42:362–5.
- Cobden I, Dickinson RJ, Rothwell J, et al. Intestinal permeability assessed by excretion ratios of two molecules: Results in coeliac disease. *Br Med J* 1978;2:1060.
- Bjarnason I, Peters TJ, Veall N. A persistent defect in intestinal permeability in coeliac disease demonstrated by a ⁵¹Cr-labelled EDTA absorption test. *Lancet* 1983;1:323–5.
- Ford RPK, Menzies IS, Phillips AD, et al. Intestinal sugar permeability: Relationship to diarrhoeal disease and small bowel morphology. *J Pediatr Gastroenterol Nutr* 1985;4:568–74.
- Juby LD, Rothwell J, Axon ATR. Lactulose/mannitol test: An ideal screen for celiac disease. *Gastroenterology* 1989;96:79–85.
- Troncone R, Starita A, Coletta S, et al. Antigliadin antibody, D-xylose, and cellobiose/mannitol permeability tests as indicators of mucosal damage in children with coeliac disease. *Scand J Gastroenterol* 1992;27:703–6.
- Bjarnason I, Maxton D, Reynolds AP, et al. Comparison of four markers of intestinal permeability in control subjects and patients with coeliac disease. *Scand J Gastroenterol* 1994;29:630–9.
- Vogelsang H, Genser D, Wyatt J, et al. Screening for celiac disease: A prospective study on the value of noninvasive tests. *Am J Gastroenterol* 1995;90:394–8.
- Uil JJ, van Elburg RM, van Overbeek FM, et al. Clinical implications of the sugar absorption test: Intestinal permeability test to assess mucosal barrier function. *Scand J Gastroenterol* 1997;223(suppl):70–8.
- Vogelsang H, Wyatt J, Penner E, et al. Screening for celiac disease in first-degree relatives of patients with celiac disease by lactulose/mannitol test. *Am J Gastroenterol* 1995;90:1838–42.
- Catassi C, Fabiani E, Ratsch IM, et al. Is the sugar intestinal permeability test a reliable investigation for coeliac disease screening? *Gut* 1997;40:215–7.
- Smecuol E, Bai J, Vazquez H, et al. Gastrointestinal permeability in celiac disease. *Gastroenterology* 1997;112:1129–36.
- Meddings JB, Sutherland LR, Byles NI, et al. Sucrose. A novel permeability marker for gastroduodenal disease. *Gastroenterology* 1993;104:1619–26.
- Sutherland LR, Verhoef M, Wallace JL, et al. A simple, non-invasive marker of gastric damage: Sucrose permeability. *Lancet* 1994;343:998–1000.
- Bjarnason Y, Macpherson A, Hollander D. Intestinal permeability: An overview. *Gastroenterology* 1995;108:1566–81.
- Meddings J. Review article: Intestinal permeability in Crohn's disease. *Aliment Pharmacol Ther* 1997;11(suppl 3):47–56.
- Van Elburg RM, Uil JJ, Mulder CJJ, et al. Intestinal permeability in patients with coeliac disease and relatives of patients with coeliac disease. *Gut* 1993;34:354–7.
- Maki M. The humoral immune system in coeliac disease. *Baillieres Clin Gastroenterol* 1995;9:231–49.
- Ferguson A, Arranz E, Kingstone K, et al. Oral tolerance, immune expression and enteropathy: Relevance to potential, latent and silent coeliac disease. In: Maki M, Collin P, Visakorpi JK, eds. *Coeliac disease. Proceedings of the seventh International Symposium on Coeliac Disease*. Tampere: University of Tampere, 1997:53–60.